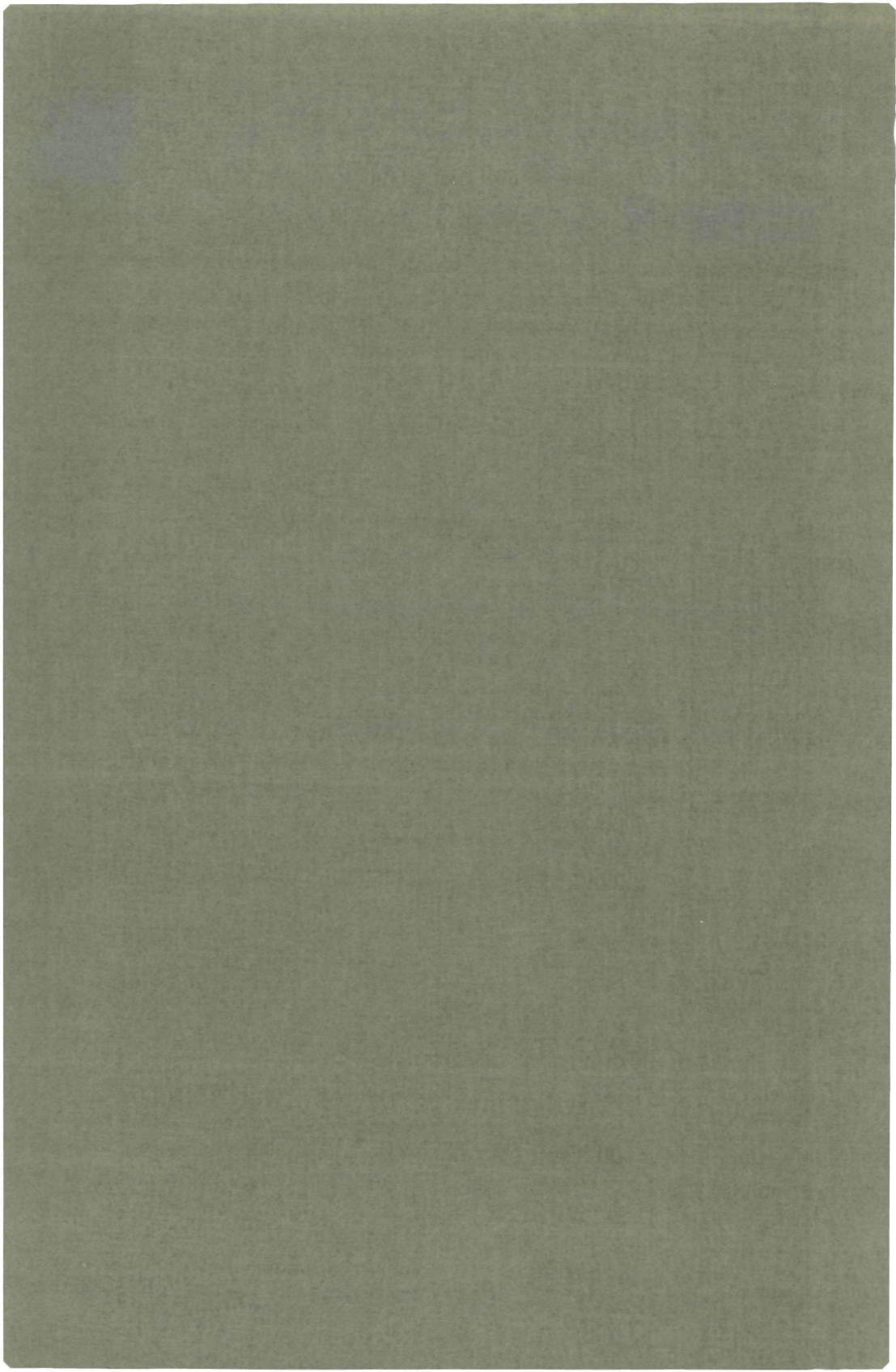


2350

HIGH-FREQUENCY PHONON EXPERIMENTS
WITH SUPERCONDUCTIVE FILMS

H. W. M. SALEMINK



**HIGH-FREQUENCY PHONON EXPERIMENTS
WITH SUPERCONDUCTIVE FILMS**

PROMOTOR
PROF DR P WYDER

CO-REFERENT
DR H VAN KEMPEN

HIGH-FREQUENCY PHONON EXPERIMENTS
WITH SUPERCONDUCTIVE FILMS

P R O E F S C H R I F T

TER VERKRIJGING VAN DE GRAAD VAN DOCTOR IN DE
WISKUNDE EN NATUURWETENSCHAPPEN
AAN DE KATHOLIEKE UNIVERSITEIT TE NIJMEGEN, OP GEZAG VAN
DE RECTOR MAGNIFICUS PROF. DR. P. G. A. B. WIJDEVELD,
VOLGENS BESLUIT VAN HET COLLEGE VAN DECANEN
IN HET OPENBAAR TE VERDEDIGEN
OP DONDERDAG 14 JUNI 1979
DES NAMIDDAGS TE 4 00 UUR

door

HUBERTUS WILHELMUS MARIA SALEMINK
geboren te Nijmegen

Druk Krips Repro Meppel

Allen, die op enigerlei wijze een bijdrage hebben geleverd aan dit proefschrift, wil ik hiervoor hartelijk danken. In het bijzonder Riki Gommers en Annie Jo Kiem Tioe, voor het verzorgen van de lay-out, en Jack Bass voor de nodige, subtiële correcties in het manuscript. Mijn dank gaat uit naar de medewerkers van de dienstverlenende afdelingen van de fakulteit der wiskunde en natuurwetenschappen en, last but not least, naar alle medewerkers van de afdeling experimentele natuurkunde 4.

Dit onderzoek werd uitgevoerd op de afdeling experimentele natuurkunde 4 van het Research Instituut voor Materialen van de Katholieke Universiteit te Nijmegen, onder leiding van Prof. Dr. P. Wyder. Een gedeelte van dit onderzoek is gesteund door de Stichting Fundamenteel Onderzoek der Materie (FOM) met financiële bijdragen van de Nederlandse Organisatie voor zuiver-Wetenschappelijk Onderzoek (ZWO).

We acknowledge the permission to reprint previously published papers, obtained from the publishers of Physics Letters, Journal de Physique and Physical Review Letters.

mijn ouders
Letje,
Maarten en Pieter.

CONTENTS

I.	INTRODUCTION	1
II.	EXPERIMENTS WITH HIGH-FREQUENCY PHONON PULSES	3
III.	EXPERIMENTAL TECHNIQUES	7
III.1.	Thin film transducers	7
III.1.1.	Evaporation techniques	8
III.1.2.	Broad-band thermal phonon transducers	9
III.1.3.	Superconductive tunnel junctions	10
III.2.	Electronic detection system	12
III.2.1.	Tunnel junction measurement and AC-modulated techniques	12
III.2.2.	Pulse generation and detection	14
III.3.	Cryogenic techniques	16
III.3.1.	He ³ -He ⁴ dilution refrigerator and experimental He-II cell	17
IV.	EXPERIMENTAL RESULTS AND ANALYSIS	21
IV.1.	Sapphire (Al ₂ O ₃)	21
IV.1.1.	Thermal phonon pulses in sapphire	21
IV.1.2.	Monochromatic phonon radiation in sapphire	28
IV.1.3.	The acoustic mismatch model	36
IV.2.	Superfluid Helium II	40
IV.2.1.	Phonon dispersion in He-II	40
IV.2.2.	Ballistic phonon pulses in liquid He-II at T < 0.35 K	44
IV.2.3.	Shock wave generation in He ⁴ gas at T = 1.2 K	50

IV.3.	Transmission of ballistic phonon pulses through a sapphire-liquid He-II interface	53
IV.3.1.	Preliminary measurements	54
IV.3.2.	Summary of experimental results	56
IV.3.3.	Analysis	60
V.	APPENDIX	86
V.1.	Thermometer calibration curve	87
V.2.	He ³ -He ⁴ mixture gas handling system	88
V.3.	He ⁴ high pressure gas handling system	89
V.4.	Tunnel junction electronics	90
V.5.	Typical second derivative trace of the I-V characteristic	91
	SUMMARY	93
	SAMENVATTING	95
	CURRICULUM VITAE	97



I. INTRODUCTION

The purpose of this thesis is to describe and discuss experiments on the transmission of pulses of ultra-high frequency sound waves (phonons) through solid dielectric crystals (sapphire), through liquid Helium at very low temperatures ($T \approx 0.1$ K) and through solid-liquid Helium interfaces (Kapitza resistance problem). In addition, the transformation of longitudinal and transverse polarized phonon pulses in the solid into the longitudinal phonon pulses in the liquid is studied for the first time. The materials investigated are so pure that the shape of the energy pulse is maintained during the propagation, due to the negligible interactions of these phonon pulses with impurities or thermal excitations (ballistic energy transport). For these experiments, fast phonon energy emitters and detectors are used with typical response-times of the order of a few nsec.

Since the pioneering heat-pulse experiments of von Gutfeld and Nethercot¹ in 1966, the phonon pulse technique has rapidly become an important tool for a number of investigations. Most of the experiments have been concerned with the intricate details of energy transport in solid dielectrics. Only a relatively small number of these high-frequency experiments has been performed to probe the energy transport in liquid Helium with its several unusual and interesting properties at low temperatures (superfluidity, second sound, anomalous dispersion). In addition, this pulse technique has been used to obtain information on the still unsolved problem of energy transfer from solids to liquid Helium, known as the Kapitza problem.

The experiments on the phonon propagation in sapphire (Al_2O_3), reported in this thesis, were performed to verify and test the experimental technique, and to provide essential data for the analysis of the experiments on solid-liquid interfaces. The experiments on ballistic phonon transport in liquid Helium at very low temperatures ($T = 0.15$ K) were devised to investigate the properties of phonon excitations in superfluid Helium. In order to study the Kapitza resistance, pulse transmission experiments through a solid-liquid interface in the ballistic regime were carried out. Under our experi-

mental conditions (very low temperatures and very pure materials), the energy propagates nearly without interaction in both materials forming the interface. In contrast to previous experiments, where the energy reflection from the solid-liquid interface was measured, in our configuration the energy transmitted into the liquid is directly determined.

This thesis is organized as follows. In sec. II, a short survey is given of the characteristics of the high-frequency phonon radiation. Some specific properties and capabilities of the phonon pulse technique are discussed. The relevant properties of some materials, which are interesting for phonon transmission experiments, are briefly reviewed. In sec. III, the experimental techniques are described. Sec. IV deals with the results and analyses of the phonon propagation experiments. Some of the reported results are reprinted from previously published papers.

REFERENCE

1. R.J. von Gutfeld and A.H. Nethercot, Phys. Rev. Lett. 12, 641 (1966).

II. EXPERIMENTS WITH HIGH FREQUENCY PHONON PULSES

Phonons are the energy quanta of lattice vibrations (sound); their energy is given by $E = \hbar\omega^*$, where ω is the frequency of the monochromatic sound wave. For a solid dielectric material, such as sapphire, the phonon frequencies range from ordinary sound frequencies up to the hypersonic range of 1000 GHz. In ultrasonic experiments, the high-frequency sound waves are transduced in the material under study by means of a generating and detecting device. Several techniques for the generation of ultrasonic waves with frequencies above 1 GHz have been reviewed by Dransfeld¹. The techniques can be divided in two categories, emitting either coherent or incoherent ultrasound. In the former group of transducers, electrical or optical generator signals are converted into high-frequency ultrasound, while maintaining the phase coherence in the acoustic wave front. These techniques include piezoelectric and magnetostrictive devices. Also the direct conversion of microwave radiation has been used for producing acoustic energy at fixed frequencies. Optical techniques, such as Brillouin and Raman scattering, have also been employed for the generation of coherent phonon radiation in solids. However, due to the imperfections in materials and interfaces, the coherent wave front readily breaks up at the high frequencies of interest (50 - 1000 GHz). Therefore, one is led to consider incoherent phonon radiation.

Incoherent techniques provide a very flexible method with general applicability. Depending on the devices used, either a broad-band or a narrow-band phonon frequency spectrum is employed. As a rather new and interesting device, superconductive tunnel junctions can be used to generate an incoherent, essentially narrow-band (mono-energetic) phonon spectrum²⁻⁴. Operation of these devices as phonon transducers relies on the fact that incident energy, larger than the superconductors gap-energy, is strongly absorbed. The minimum radiation bandwidth attainable with these devices is about 7% in the range from 120 to 870 GHz. A broad frequency spectrum can be generated by electrical or

*In this thesis the following notation is used: energy, E ; Boltzmann constant, k ; Planck constant, h , with $\hbar = h/2\pi$; phonon frequency, ω .

laser-induced pulse-heating of metallic films, which are in good thermal contact with the material to be studied⁵. The frequency distributions of these 'thermal' radiators are essentially described by a Planck-type radiation formula. These spectra have a center-frequency of $\omega_c = 3kT_h/\hbar$ with T_h being the heater temperature, and about equal spectral width. Therefore, this 'heat-pulse' technique allows only a restricted form of phonon spectroscopy. Compared with the ultrasonic work, the incoherent thermal frequencies are usually one to two orders of magnitude higher in frequency.

When the generator is heated by short pulses of typically 100 nsec duration, incoherent phonon quanta are radiated into the medium and propagate to a detector. Depending on the scattering processes in this medium and hence on the resulting phonon mean free path (mfp), the phonon flux can have the characteristics of diffusive or ballistic transport or of a collective mode (second sound). In the regime of ballistic transport, the phonon mfp is of the order of the sample dimensions (Casimir boundary scattering limit), and essentially no interactions occur within the sample. The situation can be reached in pure single crystals (Al_2O_3 , Si, Ge, NaF) at $T \approx 1$ K, and in liquid Helium-II below $T = 0.3$ K. These considerations restrict ballistic phonon pulse experiments to materials with relative long phonon mfp ($\text{mfp} \geq 1$ mm). The phonon pulses, radiated in the medium, propagate with an energy-velocity which can be different for each of the usual three phonon polarisations (longitudinal, fast and slow transverse), due to their different dispersion relations $E(k)$ and the resulting different group velocities $v_g(E) = dE/dk$. The phonon modes can be resolved due to their different time-of-flight, using a detector with a short (10 nsec) response-time. In the short generator pulses, high power densities (up to 25 W/mm^2) and resulting high phonon frequencies can be attained, without heating the entire sample. When generators and detectors of small dimensions (typically 1 mm^2) are used, a directional resolution can be obtained as well. This allows the phonon signal transmitted in a direct path, to be resolved from signals scattered at larger angles and from sidewall reflections. In contrast to this, the quantity measured in a conventional DC-thermal conductivity experiment is always an average over all phonon polarisations

and propagation directions.

The materials used in the experiments on pulsed phonon propagation reported in this work are: sapphire single crystals, superfluid Helium-II at $T = 0.15$ K, and sapphire-Helium-II interfaces at $T = 0.25$ K (Kapitza resistance). Artificial sapphire (Al_2O_3) was chosen because it provides a relatively isotropic and a pure material with little phonon scattering at the frequencies under consideration. In addition, sapphire has been studied very extensively in this type of experiments and many data are available for comparison.

Superfluid Helium-II (He-II) is a very interesting substance⁶, since it is a low temperature quantum liquid, resembling closely a Bose-Einstein condensate. Also its excitations have a unique and peculiar dispersion relation $E(k)$. Two types of single particle excitations can exist: phonons at small wavevectors, and rotons at large wavevectors; the rotons are also more localized in k -space. Because interactions among these excitations are possible, a collective energy transport mode can exist in addition to the usual diffusive or ballistic flow. Furthermore, for hydrostatic pressures below 10 bar, an unique anomalous (upward) dispersion exists for certain phonon frequencies.

The Kapitza thermal boundary resistance for energy transfer from solids to liquid He-II at low temperatures has attracted much experimental and theoretical interest in the past years⁷. Even 35 years after its discovery, it is still unclear, what mechanism is responsible for an energy transfer, which is one or two orders of magnitude larger than can be explained theoretically. Only recently, some important points in this behaviour seem to be elucidated⁸. In this thesis, experiments are reported on the transmission of phonon pulses through sapphire-liquid He-II interfaces, where phonon scattering in both materials, forming the interface, is negligible; the transfer of phonons at the interface can thus be studied in a very direct way. Therefore, this type of experiment provides a new technique for the investigation of the Kapitza resistance.

REFERENCES

1. K. Dransfeld, New directions in physical acoustics, Proc. Int. School of Physics "Enrico Fermi", Rendiconti S.I.F.-LXIII, 1974.
2. A.H. Dayem and W. Eisenmenger, Phys. Rev. Lett. 18, 125 (1967).
3. R.C. Dynes and V. Narayanamurti, Phys. Rev. B 6, 143 (1972).
4. H. Kinder, Phys. Rev. Lett. 28, 1564 (1972).
5. R.J. von Gutfeld and A.H. Nethercot, Phys. Rev. Lett. 12, 641 (1966).
6. For a review, see: H.J. Maris, Rev. Mod. Phys. 49, 341 (1977).
7. For a review, see: L.J. Challis, J. Phys. C 7, 481 (1974).
8. J. Weber, W. Sandmann, W. Dietsche and H. Kinder, Phys. Rev. Lett. 40, 1469 (1978).

III. EXPERIMENTAL TECHNIQUES

III.1. THIN FILM TRANSDUCERS

High-frequency phonons were generated and detected using evaporated thin film transducers. Two types of devices have been employed; frequency non-selective (broad-band) heaters and bolometers¹, and frequency selective superconductive tunnel junctions². Fabrication and operation of these devices is described in sec. III.1. and sec. IV.1. respectively. The propagation of phonon pulses was studied in single crystal sapphire, superfluid He-II, sapphire-He-II interfaces and in He-gas. In the study of solids, the films were evaporated directly onto the crystals (Fig. III.1.), whereas for liquid He-II they were evaporated onto glass or sapphire substrates, and the propagation medium was placed between the transducers (Fig. III.2.).

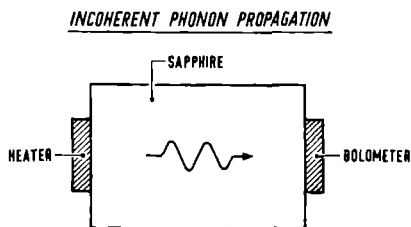


Fig. III.1. Schematic arrangement of the transducers for phonon propagation in solids.

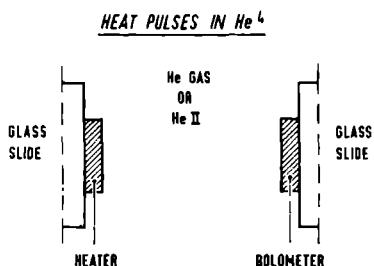


Fig. III.2. Schematic arrangement of the transducers for phonon propagation in liquid He-II or He-gas.

III.1.1. Evaporation techniques

Because of the very good thermal conductivity, sapphire crystals were mostly used as substrate material for the thin films. The substrates were used several times. Removing old and damaged films was done in acids (HCl , HNO_3), then neutralizing in a detergent (Decon) at 80°C , and finally flushing and drying with pure ethanol.

The evaporation system is an oil-free Ultek RCS system (Perkin-Elmer) equipped with three liquid nitrogen cooled (LN_2) sorption roughing pumps (Fig. III.3.). For high-vacuum operation, ion-getter, LN_2 -cryo- and titanium-sublimation pumps were used. Ultimate base pressure in the 150 l bell jar is 3.10^{-8} torr and normally the evaporation is started at 3.10^{-7} torr, attainable in about 15 min. after the pump cycle is started. An Airco-Temescal 8 kW electron beam gun is used as evaporation source. The thickness of the evaporated films is measured with a crystal-quartz-controlled Kronos ADS-200 system, also

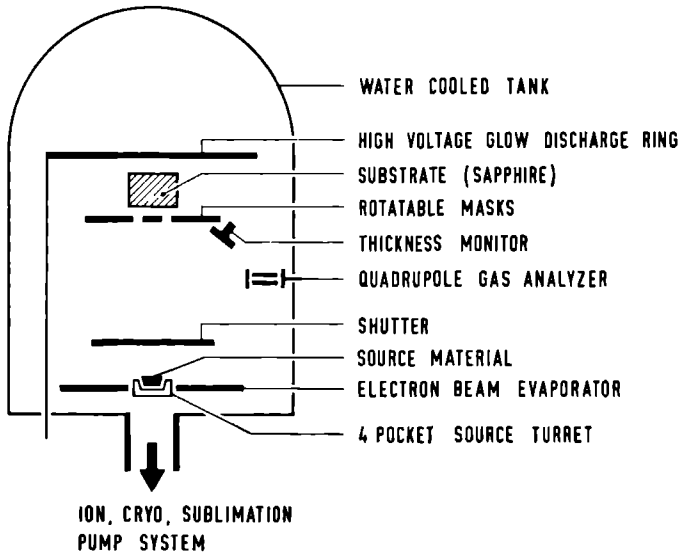


Fig. III.3. Evaporation system.

used to regulate carefully the deposition rate to within 0.1 nm/s. Calibration of this thickness monitor was done with the aid of an optical interferometer (Varian A-scope) with a thickness accuracy of 3 nm. Typical evaporation parameters for the most frequently used materials are given in Table III.1.

Table III.1.

material	thickness (nm)	deposition rate (nm/s)	evaporation pressure (torr)	electron beam current (A)
Al	15-25	1.0- 5.5	8.10^{-7}	0.25-0.30
Sn	25-55	2.5-10	2.10^{-6}	0.23-0.27
Si	50	0.2- 0.5	3.10^{-7}	0.10
SiO ₂	50	0.2- 0.5	5.10^{-7}	0.04
constantan	15-18	0.2- 0.5	5.10^{-7}	0.30

The acceleration high-voltage was mostly 10.5 kV. For Si and SiO₂ an electron beam X-Y sweep was used. With the exception of constantan, these materials were evaporated without crucible liners.

A nitrogen (N₂) glow-discharge was released at a pressure of 0.1 to 1 torr during the pump-down from atmospheric pressure, in order to clean the substrates and to improve film adherence. For the production of some films (notably thin Pb), the substrate was cooled to 85 K, but otherwise the substrate temperature was measured to be between 30 and 80°C.

III.1.2. Broad-band thermal phonon transducers

For the generation of thermal phonon pulses, a thin resistive heater of a disordered alloy (constantan) was used. Typical film dimensions were an area of 1x1 mm² and a thickness of 15 nm. This resulted in a film resistance of 50 Ω, providing a good power matching to the electrical circuitry with its characteristic impedance of 50 Ω. The characteristics of the phonon radiation of these films are discussed in sec. IV.1.

The phonon detectors consisted of similarly dimensioned metallic thin films of Al, Sn or In, with a somewhat wider range of thicknesses (15 - 55 nm). These films became superconducting below their (zero-field) transition temperature (T_c) and hence have a high temperature sensitivity in the resistance (dR/dT) at T_c . The resistance in the normal state varies from 30 to 250 Ω , depending mainly on film thickness and evaporation rate. Operation of these detectors at $T = T_c$ is obviously very restricted and demands a rather good temperature stabilisation. For operation at temperatures $T < T_c$, the detectors were placed in a parallel magnetic field to bring the film to its magnetic field transition (H_c). A 4.0 T superconducting magnet of high homogeneity³ was used for this purpose. The fast thermal response of these evaporated thin films is due to the good thermal conductivity K to the substrate and the very low heat capacity C . The resulting thermal response times $\tau = K.C$ are of the order of 10 - 30 nsec^{1,4}.

III.1.3. Superconductive tunneling junctions

The superconductive tunneling junctions were prepared in the form of crossed stripes separated by a thin layer of natural grown oxide of thickness of 1.5 to 3.5 nm (Fig. III.4.)⁵. The junctions were fabricated in one vacuum run, using stainless steel masks to determine the

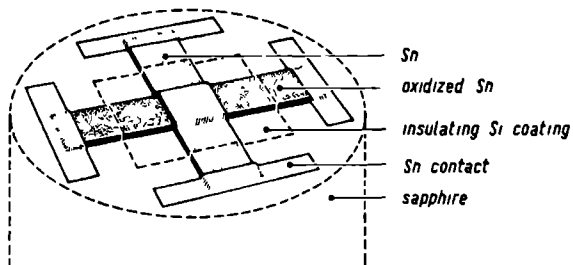


Fig. III.4. Thin film superconductive tunnel junction.

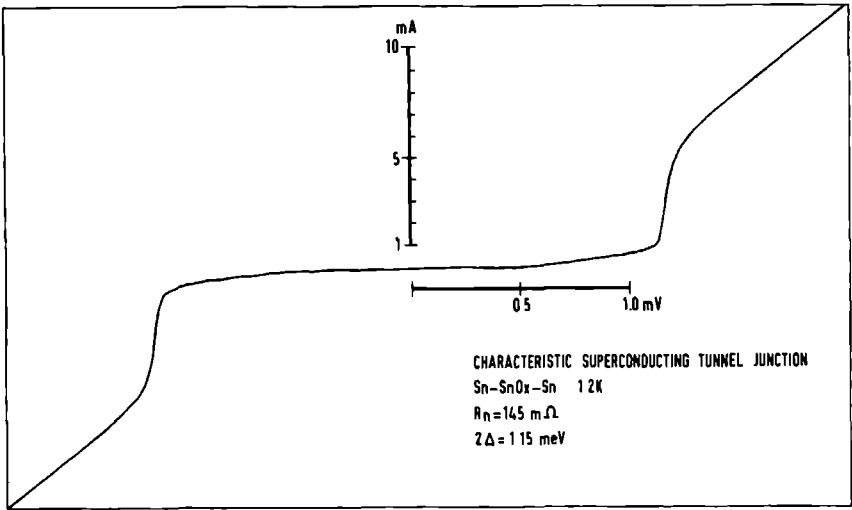


Fig. III.5. Current-voltage (I-V) characteristic of a Sn-Sn tunnel junction.

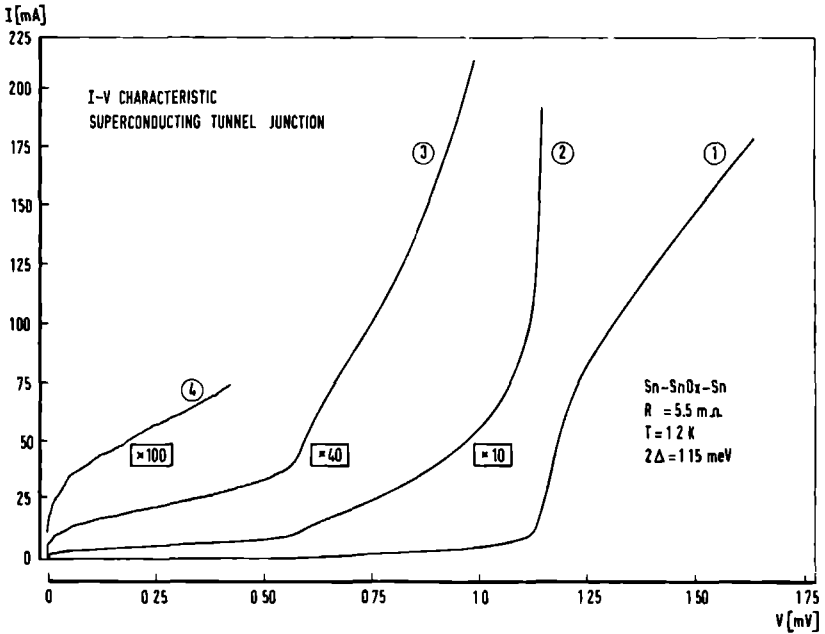


Fig. III.6. I-V characteristic of a Sn-Sn tunnel junction, showing several tunneling processes (Refs. 6 and 7). The traces 2,3 and 4 are amplifications of trace 1, as indicated.

film width: 0.15 to 1.5 mm. The materials used were Al, Sn or granular (oxygen-doped) Al:O. The Al:O junctions were made by evaporating aluminum at slow rates (0.5 - 1.0 nm/sec) in a high O₂ background pressure of about 10⁻⁴ torr. The film thickness was between 55 and 250 nm. Connection to the junction was made with 350 nm thick contact areas of Sn (Fig. III.4.), where In-coated leads were pressed upon. This resulted in low-ohmic, very reliable contacts. The insulating layer was formed by oxidation in pure O₂ at a pressure of 0.1 to 1.0 torr, employing a moderate glow discharge to improve the insulator growth. The normal state resistances of the Sn junctions were between 5 and 150 mΩ, those of the Al junctions between 0.1 and 1 Ω. In some cases, thin (55 nm) silicon layers were evaporated over the entire junction to improve the cyclability to room temperature and the resistance to atmospheric conditions. No effect on the characteristics was observed.

Typical current-voltage (I-V) characteristics of Sn-Sn junctions are shown in Figs. III.5. and III.6. In Fig. III.6. it is seen that in these low-ohmic junctions other tunneling processes than simple single particle tunneling can take place as well: the increase in current at 2Δ/e origins from two-particle tunneling⁶, and the constant voltage steps at low voltage results from resonance of the AC-Josephson current in the junction cavity⁷. The junctions were always measured in a four-terminal circuit.

III.2. ELECTRONIC DETECTION SYSTEM

III.2.1. Tunnel junction measurement and AC-modulation techniques

The electronic equipment used for recording I-V characteristics of the tunnel junctions and the first (dI/dV) and second derivative (d²I/dV²) as a function of voltage was a modification of the apparatus described by Adler and Jackson⁸. It consists of a DC-current supply, an AC-current modulator, and a suitable resistance bridge network. The DC-current can be swept slowly over a range of -1 A to +1 A. A small AC-current modulation with a frequency of 0.5 kHz and an amplitude up to 1 mA can be superimposed. To avoid grounding problems,

BLOCK DIAGRAM MODULATED DC EXPERIMENT

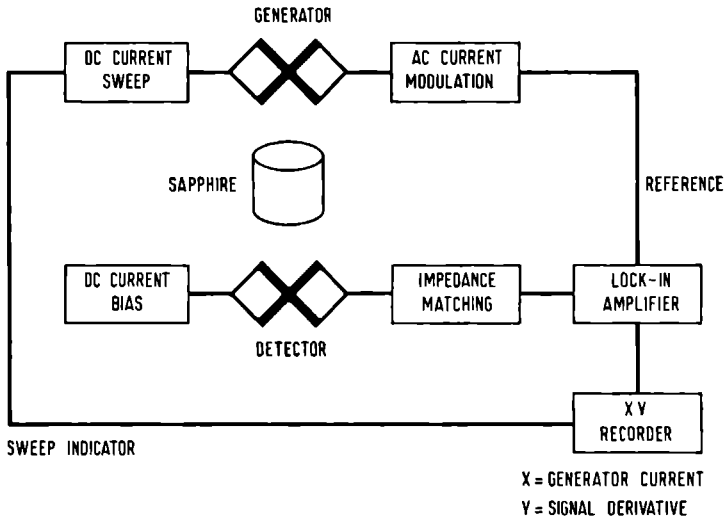


Fig. III.7. Block diagram for AC-modulated, monochromatic phonon transmission experiment.

BLOCK DIAGRAM TIME-OF-FLIGHT EXPERIMENT

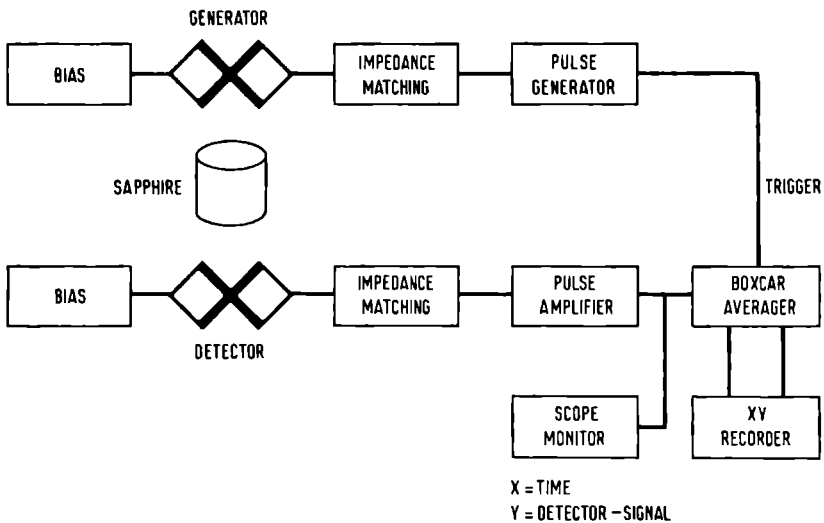


Fig. III.8. Block diagram for pulsed phonon transmission experiment.

the modulator is fed from rechargeable batteries. The resulting DC-voltage from the junction is directly fed to the X-axis of an XY-recorder (Hewlett-Packard 7047A), whose Y-axis is driven by a voltage proportional to the DC-current. The AC-voltage from the junction is phase-sensitively detected at 0.5 kHz using a PAR HR-8 lock-in amplifier. For measurements of the second derivative, the AC-voltage from the junction is detected at 1.0 kHz (second harmonic) by a PAR 186 lock-in amplifier. By compensating the DC-resistance of the junction in the resistive bridge circuit, the lock-in is able to detect small changes in the AC-measurements.

For the measurements on AC-modulated phonon generation, described in sec. IV.1.2., the detection scheme of Fig. III.7. is used. Two tunnel junctions evaporated opposite each other on a cylindrical substrate are employed, one as the generator, the other as detector. The generator is driven by a slowly swept DC-current to raise its excitation voltage, with a small AC-current superimposed. The resulting detector voltage is phase-sensitively amplified and the derivative of the received phonon signal, with respect to generator voltage, is directly recorded. In this case a PAR 190 or AM-1 transformer was used to match the low junction impedance ($< 1 \Omega$) to the amplifier input resistance. A PAR 113 low noise preamplifier and one of the lock-in amplifiers of the types mentioned above were used. Typically, in these measurements the noise level was 2.5 times the thermal noise and limited by spurious RF interference.

III.2.2. Pulse generation and detection

The electronic set-up for generation and detection of phonon pulses is shown in Fig. III.8. Current pulses are supplied to the generator film by a Hewlett-Packard 8015A pulse generator. For higher powers, an E-H model 133A generator was used¹¹. Typically, the following pulse parameters were used: pulse width of 50 - 150 nsec, rise- and falltimes of 15 - 30 nsec, and repetition rates ranging from 1 Hz to 1 kHz, depending on the allowed energy dissipation; the pulse amplitudes were between 0.5 and 15 V over 50 Ω film resistances of the heater. The films were connected with 50 Ω miniature coaxial cables

to the electronic equipment, with an overall bandwidth of 35 MHz. When tunnel junctions of low impedance ($< 1 \Omega$) were used, impedance matching was provided by a 1:7 ratio pulse transformer with a 15 nsec risetime, and a stripline with a characteristic impedance of 1Ω . A capacitor was used in the primary circuit to block the DC-current. Accurate and reproducible pulse amplitude settings were obtained by maintaining a fixed generator amplitude and a variable RF step attenuator (Telonic 8143A). The attenuated generator pulse was monitored via a RF tap-off (EH 960) and a Tektronix 7704 oscilloscope. For short delay times between the generator pulse and the signal to be detected, electro-magnetic cross-talk from the generator pulse could cause problems with the signal recovery. In most cases, this effect could be minimized to an adequate low level by proper impedance matching, shielding and grounding, or by properly adjusted pulse parameters on the generator (rise- and falltime and pulse width).

The superconductive detector film is operated mostly at the magnetic transition (H_c). The high temperature-sensitivity of the resistance (dR/dT) is sensed by a small DC-bias current, delivered by a mercury battery (Mallory) via a suitable metal-film load resistor. The signals are always increasing linearly with bias current in the range used (10-120 μA). The resulting small detector signal pulses (0.1 to 10 μV) are AC-coupled (via a capacitor) to low-noise, wide-band RF amplifiers⁹, providing about 60 db total gain. In cases of severe noise or interference, bandwidth limitation was provided in the amplifier stage by means of suitable low-pass filters with cut-off frequencies from 15 to 35 MHz. The amplified signals were averaged in a PAR model 160 boxcar integrator whose output is plotted on an XY-recorder. After averaging, a system risetime of 15 nsec was maintained with a noise level of less than 0.5 μV in a 35 MHz bandwidth.

In the low-temperature experiments at $T = 0.1$ K, where the pulse repetition rate has to be low (1 to 25 Hz) due to the limited cooling power available ($\approx 10 \mu W$), the boxcar averager was replaced by a Biomation 8100 transient recorder (Fig. III.9), which digitizes the signal, with 8 bit amplitude resolution and 10 nsec time resolution, over a 20 μsec time interval. This information (2000 8-bit words) is then transferred to a digital signal averager (Tracor Northern 570A)

BLOCK DIAGRAM TIME-OF-FLIGHT EXPERIMENT

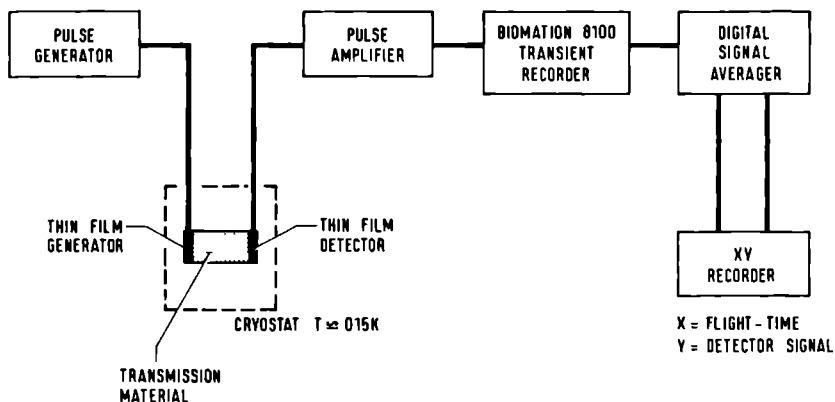


Fig. III.9. Block diagram for pulsed phonon transmission experiment using digital signal acquisition.

for accumulation of successive digital recordings. Up to 16,000 sweeps could be averaged in this way in four independent memories, and some simple arithmetic could be performed. If it was necessary to suppress the generator pulse crosstalk, the signals from carefully adjusted generator pulses, of equal amplitude but of opposite polarity, were recorded. Bandwidth limitation was always used to prevent erroneous effects of frequencies above 25 MHz in the digitizing process. As a more flexible alternative for the digital signal processing, a PDP-12 processor could be used via an interface to the Biomation recorder.

III.3. CRYOGENIC TECHNIQUES

The experiments at $T = 1.2$ K were performed with the samples and the films or junctions directly immersed in a pumped liquid He-II bath. Coaxial cables or low-impedance strip-lines were used to connect the films to the electronic equipment.

III.3.1. He³-He⁴ dilution refrigerator and experimental He-II cell

The experiments at a temperature of $T = 0.1$ K were performed in a simple home-built dilution refrigerator¹⁰. This system is schematically shown in Fig. III.10. Precooling and condensing of the circulating He³ gas takes place in the He⁴ bath, which is pumped to $T = 1.5$ K. The necessary refilling of this bath was the limiting factor in the continuous operation of the machine. The gas handling system for the He³-He⁴ mixture is shown in the appendix. The cooling power of the refrigerator was $15 \mu\text{W}$ at a temperature of $T = 0.1$ K, using a Helium-sealed Alcatel 2060H two stage rotary pump.

The actual experiments were performed in a stainless steel pressure cell, with a diameter of 35 mm and a volume of 30 cm^2 , attached to the mixing chamber of the refrigerator. Heat exchange was provided by a copper rod, with direct access to both chambers; each end of the rod has some 50 cm^2 of copper finned area. The experimental cell has a detachable stainless steel flange at the bottom, on which the different parts of the experiments could be assembled. It was fastened by 16 bolts and sealed by a simple Indium-O-ring construction.

For the experiments of phonon pulse transmission from sapphire to liquid He-II (sec. IV.3), a special flange was constructed. In this construction the heater film was isolated from the liquid He-II by placing it in the vacuum space of the refrigerator. This assembly is shown in Fig. III.11 and it is described in more detail in sec. IV.3.3. The He-II cell could be filled with pure (5N5) liquid Helium for cooling the samples or for providing the propagation medium for the phonon pulses (see sec. III.1 and sec. IV.2 and IV.3). This Helium was condensed from a closed He⁴ gas system, after passing over liquid nitrogen (LN_2) cooled traps. The He⁴ gas handling system is shown in the appendix. By means of this gas system, the He-II liquid in the cell could be pressurized up to the solidification point of 25.5 bar at $T = 0.1$ K.

The temperature in the He-II cell was monitored by means of a Speer carbon resistor in an AC Wheatstone bridge circuit, using a lock-in amplifier as a null detector. The resistor was calibrated against a

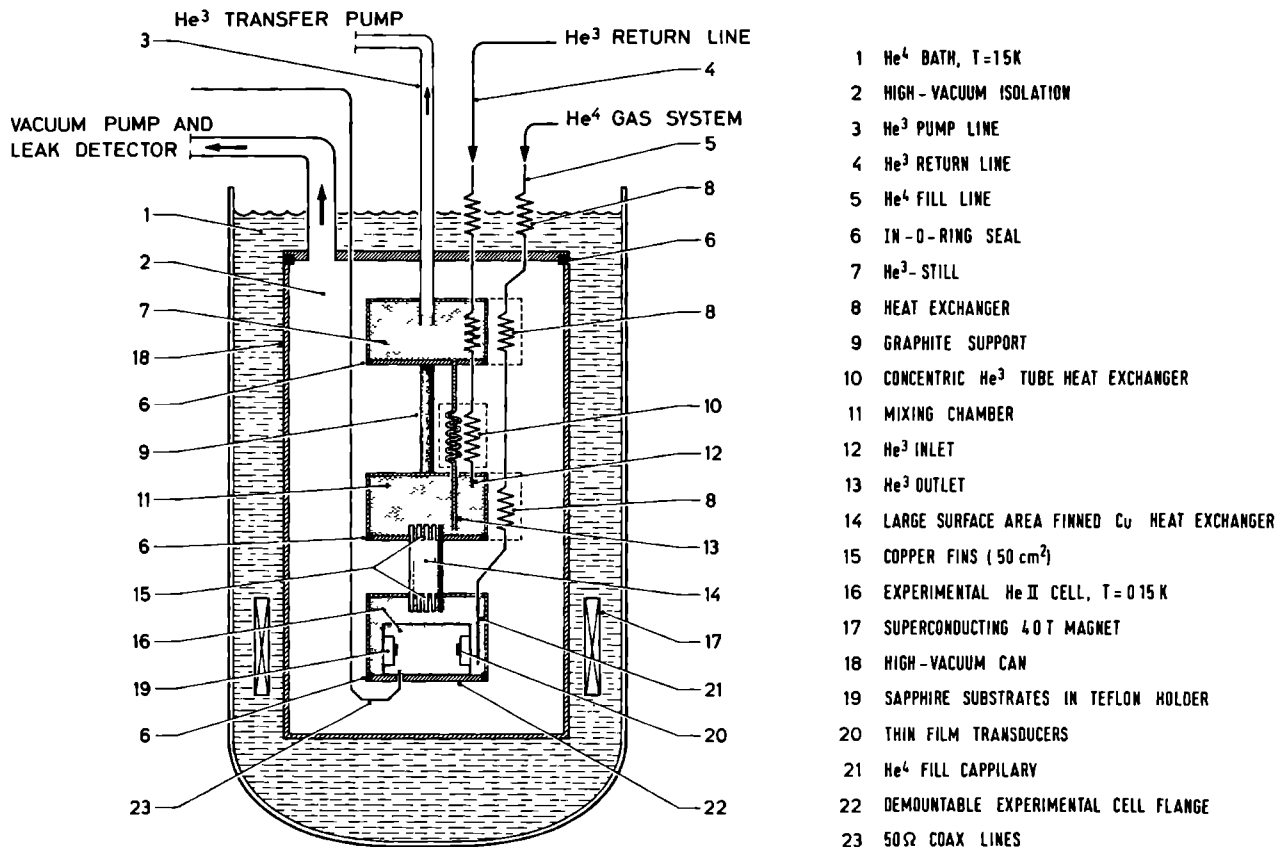


Fig. III.10. Schematic arrangement of He³-He⁴ dilution refrigerator and experimental He-II pressure cell. The dewar with liquid nitrogen is omitted for clarity.

CMN susceptibility thermometer; the calibration curve is also shown in the appendix. Temperature regulation was obtained by connecting the null-detector output to a current feedback regulator and a heater in the cell. The uncertainty in the temperature is 5 mK below $T = 300$ mK. The error in temperature, due to the magnetoresistance of the carbon resistor is about 15 mK, but this is still sufficiently small for our purposes. For operation of the superconductive film detector at the magnetic transition at reduced temperatures, a superconducting magnet of 4.0 T was installed³. The films were connected to the measurement circuitry by means of six miniature coaxial cables of 50 Ω impedance.

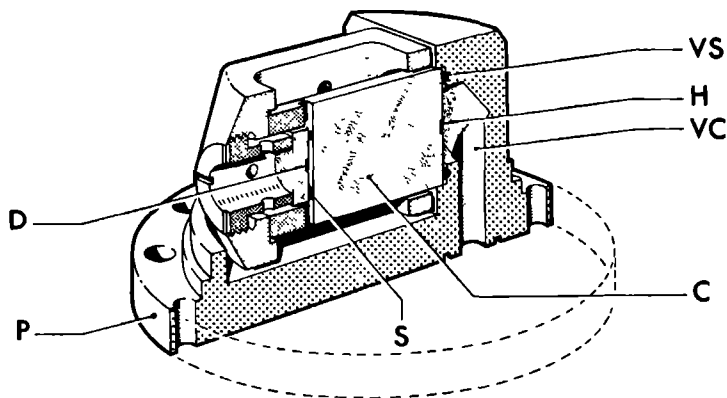


Fig.III.11. Cut-away view of the flange of the He-II cell, showing the construction of the vacuum-isolated heater film. The letters refer to: P, pressure cell flange; D, detector film; S, spacer between crystal and detector; C, sapphire crystal; VS, vacuum seal with Indium-O-ring; H, heater film; VC, connection to vacuum chamber of the refrigerator.

REFERENCES

1. R.J. von Gutfeld and A.H. Nethercot Jr., Phys.Rev.Lett. 12,641 (1964).
2. A.H. Dayem and W. Eisenmenger, Phys.Rev.Lett. 18, 126 (1967).
3. The magnet was manufactured by Cryogenic Consultants, London.
4. R.J. von Gutfeld, A.H. Nethercot and J.A. Armstrong, Phys.Rev. 142,436 (1966).
5. I.Giaever, Phys.Rev. Lett. 5,464 (1960).
6. J. Wilkins, in Tunneling phenomena in solids, edited by E.Burstein and S. Lundqvist (Plenum Press) 1969.
7. M. Fiske and D. Coon, Phys.Rev. 138A,744 (1965).
8. J.G. Adler and J.E. Jackson, Rev.Sci.Instr. 37,1049 (1966).
9. The low-noise RF amplifiers were manufactured by Avantek; the types used were : AWL-500 and AV9T.
10. H.E. Hall, P.J. Ford and K. Thompson, Cryogenics 6,80 (1966).
- 11 A Hewlett-Packard 9016A pulse generator was most generously lent to us for some time by the group of Atomic and Molecular physics of Prof. Dymanus.

IV. EXPERIMENTAL RESULTS AND ANALYSIS

This chapter contains the results of ballistic phonon experiments in sapphire, liquid He-II, and of phonon transmission experiments in sapphire-He-II interfaces at $T \leq 0.25$ K. This last experiment was attempted to provide an alternative technique for the study of energy transport in solid-He-II interfaces by measuring direct phonon transmission with high time-resolution and ballistic propagation in both media forming the interface. The experiments in sapphire and liquid He-II are necessary for knowledge of the phonon propagation characteristics in these two materials. The relevant features of the acoustic mismatch model (AMM) are discussed in sec. IV.1.3.

IV.1 SAPPHIRE (Al_2O_3)

IV.1.1 Thermal phonon pulses in sapphire

Synthetic sapphire (Al_2O_3) has often been used in phonon pulse experiments as it provides a rather 'transparent' medium for the high phonon frequencies involved (100-500 GHz)¹⁻⁵. Acoustic dispersion can be neglected in the longitudinal (L) and transverse (T) phonon branches up to 1 THz (linear dispersion)^{6,7}. For the temperatures T_h used in the heater, ($T_h \leq 15$ K), the emitted phonon frequency distributions are not influenced by velocity dispersion^{1,6,7}, so all frequencies propagate with the same velocity. Sapphire can be manufactured with a high degree of physical and chemical purity, and it has a high Debye temperature of 980 K compared with the phonon energies used. The high Debye-cutoff frequencies (3 THz) do not influence the phonon frequency spectra for heater temperatures of 15 K and these distributions can be calculated with a Planck type radiation expression using an acoustic mismatch model⁸ (AMM), see sec. IV.1.3. Also sapphire has a low isotope scattering rate for the phonon frequencies used. A phonon mean free path of 10 nm for 100 GHz phonons can be obtained for $T < 2.5$ K (Casimir boundary scattering regime)⁹. High quality Verneuil (V) or Czochralski (CZ) grown single crystal sapphires with a dislocation

density of less than $10^3/\text{cm}^2$ were used in the phonon transmission experiments¹⁰. The crystals were cylinders of diameters of 10 and 15 mm and lengths of 8, 10, 15 and 20 mm respectively. Generator and detector films of 1 mm^2 area were evaporated on the flat surfaces, accurately aligned with respect to each other. The cylindrical axis was parallel to a high-symmetry crystal direction within 1.5° . With the phonon propagation path parallel to the crystallographic a-axis, the three phonon modes, longitudinal (L) and fast and slow transverse (FT resp. ST), can be resolved, due to their different ultrasonic velocities¹¹, by their arrival time following an excitation pulse. In the c-axis direction the two transverse modes are degenerate in velocity¹¹, and only an L and a merged T mode pulse are observed, apart from possible sidewall reflections. The detected time-of-flight signal in a c-axis sapphire is shown in Fig. IV.1.

A constantan heater and a superconductive aluminium detector film, used as a bolometer, were employed in this experiment. To achieve a high temperature coefficient of the resistance (i.e. a high sensitivi-

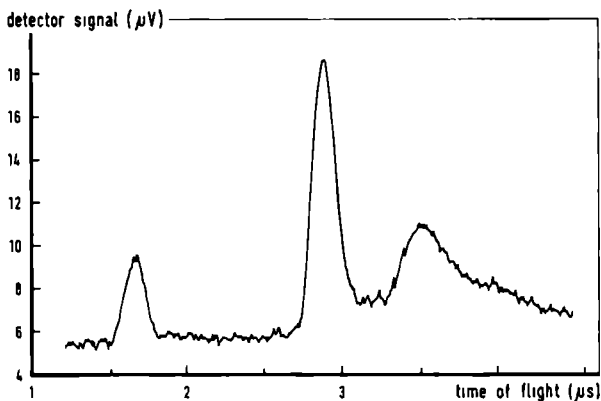


Fig. IV.1. Time-of-flight signal in a c-axis sapphire using (thermal) broad-band phonon transducers (Crystal length: 15 mm, diameter: 15 mm, excitation pulse width: 150 nsec, pulse power density: $67\text{ mW}/\text{mm}^2$).

ty, dR/dT) these aluminium films were current biased at their superconductive resistance transition: either at the zero-field transition temperature T_c , or for $T/T_c < 1$, at their parallel critical field $H_{c\parallel}$. In this last case, very stable signals were obtained. The magnetic field was produced by a superconducting magnet (see also sec. III). Due to the low heat capacity and the good thermal contact to the substrate, the response-time of these films of 15-35 mm thickness is typically of the order of 10-25 nsec¹². The phonon spectra, emitted by the generator film, contain a broad-band, black-body type frequency distribution¹³. The characteristic instantaneous heater temperature T_h and the associated phonon spectra can be calculated from the absorbed power density using a modified acoustic mismatch model^{7,8}.

Assuming thermal equilibrium between electrons and phonons within 10 nsec, a modified isotropic Debye model for heater and propagation medium and a substrate temperature of $T = 0$ K, the resulting phonon spectra have been calculated by Weis⁸. The spectral power distribution $P(\omega, T_h)$ emitted from the generator into the crystal is then given by a Planck type formula:

$$\frac{P_m(\omega, T_h)}{A} = \frac{\hbar}{8\pi^2} \left(\frac{e_m}{c_m^2} \right) \frac{\omega^3}{\exp(\hbar\omega/kT_h) - 1} \quad (1)$$

Here, A is the heater film area, m the phonon polarisation-index (L or T), e_m the phonon transmission coefficient from film to substrate for mode m , c_m the ultrasonic phase velocity (ω/k) for mode m , k the Boltzmann constant and h the Planck constant, with $\hbar = h/2\pi$ ⁸. In the limit of $T_h \ll \Theta_D$ (the Debye cutoff temperature; 390 K for constantan), the relation of the heater temperature to the power density is given by integrating (1) over all frequencies. This results in:

$$\frac{P_m(T_h)}{A} = \frac{\pi^2}{120 h^3} \left(\frac{e_m}{c_m^2} \right) (kT_h)^4 \quad (2)$$

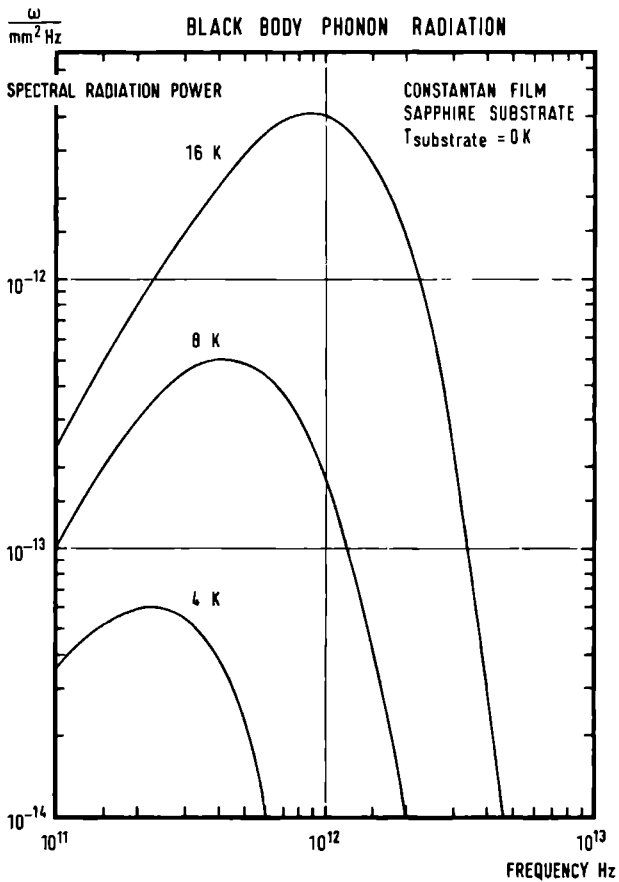


Fig. IV.2. Calculated black-body frequency spectrum for a constantan film at different temperatures T_h , on a sapphire substrate at $T = 0^{\circ}\text{K}$. The drawn distributions refer to the indicated heater temperatures (after Weis, Ref.8).

This resembles the Stephan-Boltzmann law for black-body radiation. The total power density in both modes is then ($m = L, T$):

$$\frac{P(T_h)}{A} = \frac{\pi^2}{120 h^3} \left(\frac{e_L}{c_L^2} + \frac{2e_T}{c_T^2} \right) (kT_h)^4 \quad (3)$$

which is used for a calculation of the heater-temperature T_h . Estimates of the transmission coefficient for a constantan-sapphire interface from the acoustic mismatch model (AMM) are $e_L = 0.22$ and $e_T = 0.17$ ⁸. The effect of a non-zero substrate temperature (T_0) can be included in Eq. (3), by adding a term in T_0 similar to that for T_h . The calculated frequency spectrum for constantan on sapphire at $T_0 = 0$ K is shown in Fig. IV.2. As in the electromagnetic black-body radiation, the dominant frequency (ω_m) is given by $\hbar\omega_m = 2.82 kT_h$, or $\nu = \omega/2\pi = 59.T_h$ (GHz), where T_h is measured in K. The radiation-bandwidth at frequencies of half the intensity maximum is about equal to ν_m . For heater temperatures up to about $T_h = 15$ K (the maximum temperature used in our experiments) the emitted spectra have been experimentally verified to be described by a black-body radiation, assuming that the AMM is applicable¹³.

For power levels up to 3.0 W/mm^2 , a linear dependence of signal intensities on pulse power density and on pulse length (pulse energy) is found. This indicates a broad-band energy detection mechanism (bolometric response). The signal intensity increases linearly with detector bias current in the range used (10-100 μA). For phonon propagation along the c-axis in sapphire, the intensity ratio of the L and T mode pulses (L/T ratio) is found to be 0.30 ± 0.03 , in accordance with theoretically calculated values¹⁴. For c-axis sapphire, the phonon velocities are $10.2 \cdot 10^3$ m/s for the L mode and $6.05 \cdot 10^3$ m/s for the T mode. The time-of-flight signal for a 50 nsec long excitation pulse in an 8 mm long c-axis sapphire is shown in Fig. IV.3. A constantan heater (15 nm thick) and an aluminium detector (18 nm thick) were used. This signal shows the fast thermal response time (smaller than 25 nsec) attainable with these thin films.

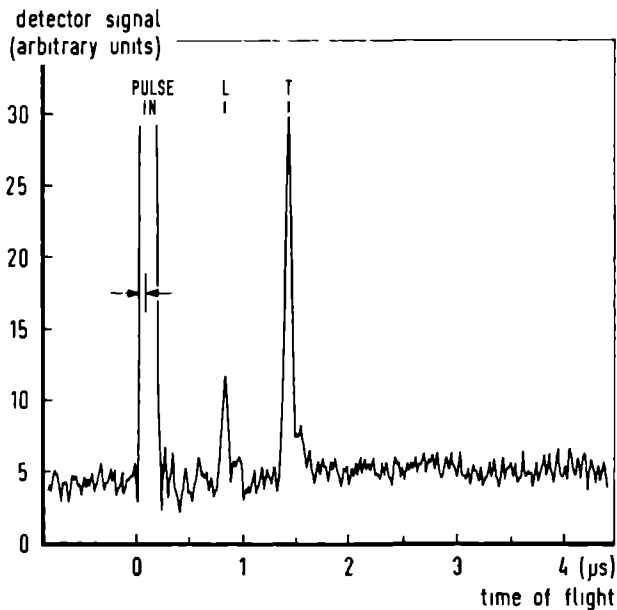


Fig. IV.3. Detected ballistic phonon signal in a c-axis sapphire using broad-band transducers (Crystal length: 8 mm, diameter: 15 mm, excitation pulse width: 50 nsec, pulse power density: 20 mW/mm²). The generator pulse width is indicated by arrows.

REFERENCES

1. R.J. von Gutfeld and A.H. Nethercot, Phys. Rev. Lett. 12, 641 (1964).
2. A.H. Dayem and W. Eisenmenger, Phys. Rev. Lett. 18, 125 (1967).
3. O. Weis, Acustica 21, 162 (1969).
4. B. Taylor, H.J. Maris and C. Elbaum, Phys. Rev. B3, 1462 (1971).
5. H. Kinder, Phys. Rev. Lett. 28, 1564 (1972).
6. H. Bialas and H.J. Stolz, Z. Phys. B21, 319 (1975).
7. P. Herth and O. Weis, Z. Angew. Phys. 29, 101 (1970).
8. O. Weis, Z. Angew. Phys. 26, 325 (1969).

9. H. Salemink, doktoraalscriptie, University of Nijmegen, Exp. Nat. 4 (1973).
10. The sapphire single crystals were supplied by:
 Adolf Meller, Providence, Rhode Island, U.S.A.
 Union Carbide, San Diego, California, U.S.A.
11. R.J. von Gutfeld, Physical Acoustics Vol. V-6, ed. W.P. Mason, p. 233.
12. R.J. von Gutfeld, A.H. Nethercot and J.A. Armstrong, Phys. Rev. 142, 436 (1966).
13. W.E. Bron and W. Grill, Phys. Rev. B16, 5303 (1977).
14. F. Rösch and O. Weis, Z. Phys. B29, 71 (1978).

IV.1.2. Monochromatic Phonon Radiation in Sapphire

A narrowband phonon transducer system can be realized by employing a set of two identical thin-film superconductive tunnel junctions (STJ) as generator and detector¹⁻⁴.

The energy gaps at $T = 0$ K of the superconductors most commonly used in this type of experiment are listed in Table IV.1. for different energy units.

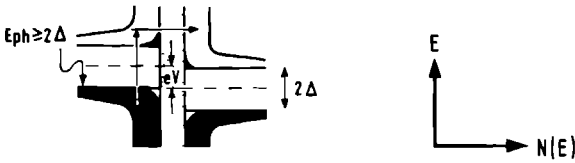
Table IV.1.

Material	T_c (K)	Energy gap (2Δ)			
		meV	GHz	K	cm^{-1}
Al	1.2	0.30	90	4.3	3
Al:O	1.5-1.8	0.37	120	5.2	4.2
Sn	3.8	1.15	280	13.2	12
Pb	7.2	2.80	680	34	22

The Al:O junctions are evaporated in a high oxygen background pressure (10^{-4} torr) to obtain granular films.

For our purposes, the phonon radiation characteristics of a STJ are described adequately by simple semiconductor type diagrams as shown in Fig. IV. 4 and Fig. IV.5. The energy (E) is plotted (vertically) against the density-of-states (horizontally) for the three materials forming the STJ sandwich, showing the BCS singularity in the density-of-states adjacent to the energy gap. This picture is not adequate in the sense that it assumes the occupied levels to be condensed Cooper pairs (following Bose statistics) and the empty states to be single quasi-particles (following Fermi statistics). These problems are treated correctly in the well-known $E(k)$ diagrams introduced by Schrieffer⁵. The intensity of the tunnelcurrent depends upon the particle densities in the occupied and allowed energy states in the respective films and upon the effectiveness of the tunnel barrier (Fermi's golden rule) for elastic tunneling processes. For a junc-

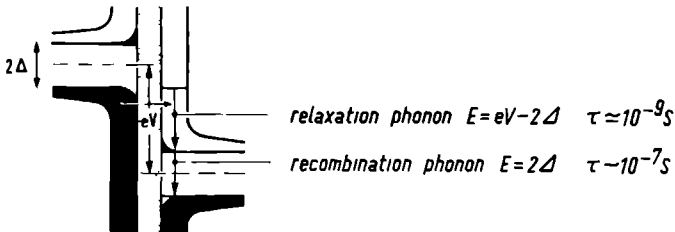
PHONON DETECTION $0 < eV < 2\Delta$
 BY PAIR-BREAKING



ENERGY VS DENSITY OF STATES DIAGRAM
 BLACK=OCCUPIED ENERGY LEVELS

Fig. IV.4 Energy vs density of states diagram for a superconductor-insulator-superconductor tunnel junction. Detection of phonon energy $\hbar\omega > 2\Delta$ is optimal for $eV < 2\Delta$.

PHONON GENERATION $eV > 2\Delta$
 BY INJECTED QUASI-PARTICLE DECAY



ENERGY VS DENSITY OF STATES DIAGRAM
 BLACK=OCCUPIED ENERGY LEVELS

Fig. IV.5 Energy vs density of states diagram for a superconductor-insulator-superconductor tunnel junction, showing phonon generation by the relaxation and the recombination process.

tion biased at a voltage $V < 2\Delta/e$ (leading to an energy difference of eV between the two Fermi-levels), a small quantum-mechanical tunnel current flows at $T/T_c < 1$, due to the thin insulating oxide (1-3 nm) layer and the residual thermal electrons in the tails of the Fermi distribution at $eV-\Delta$ (upper gap edge) (Fig. IV.4).

Detection of phonon energy $\hbar\omega > 2\Delta$ is accomplished by 'breaking' Cooper pairs in the second film, forming excitations above the gap. This population-increment above the gap results in an increase in the thermal tunneling current, effected by the voltage $V < 2\Delta/e$ over the junction. The frequency dependence of the sound adsorption in superconductors was calculated by Bobetic⁶ using a BCS model; these results are plotted in Fig. IV.6.

If the film thickness is larger than the phonon mean free path, such a junction will effectively absorb only high-frequency phonons of energy $\hbar\omega > 2\Delta$. Therefore, the junction possesses a frequency selective high-pass property.

Phonon generation in superconductive tunnel junctions can be explained by using Fig. IV.5 and a three level model^{1,2}.

level 0, the ground state below the energy gap consisting of condensed pairs, level 1, the first possible excitation level of quasi-particles, separated from the groundstate by the energy gap 2Δ ; level 2, the injection level, eV in energy above the ground state, determining the maximum energy of the tunneling quasi-particles. As can be seen from Fig. IV.5, quasi-particles tunnel from occupied states in one film into empty states in the other. In this 'receiving' film, these particles are 'superthermal', and in the de-excitation process towards thermal equilibrium, their excess energy is radiated away, mainly by phonon emission⁷. Two distinct de-excitation processes occur in a superconductor. The first step is the relaxation from the injection level (between eV and 2Δ above the ground state) to the upper gap edge (level 1), which yields a phonon energy ($\hbar\omega$) between 0 and $eV-2\Delta$. The second step is the recombination of two opposite spin particles to one Cooper pair in the condensed state (level 0), emitting a phonon with energy-

ULTRASONIC ABSORPTION IN A BCS SUPERCONDUCTOR

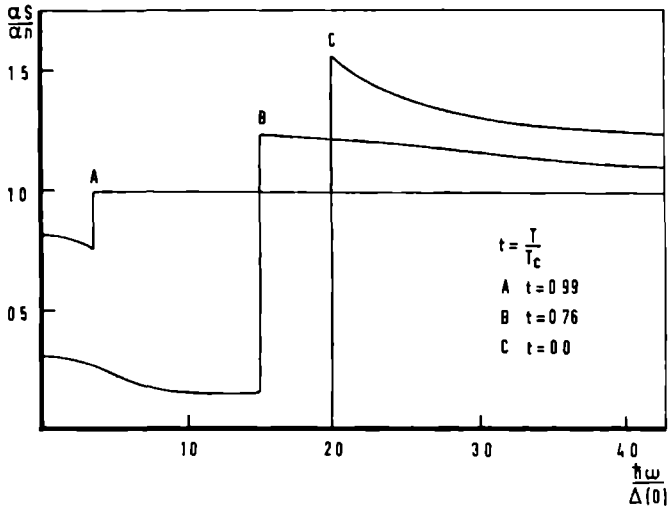


Fig. IV.6. Calculated high-frequency sound absorption in a superconductor as a function of frequency (after Bobetic, Ref. 6).

EMITTED PHONON SPECTRUM FROM BCS SUPERCONDUCTOR
(CALCULATED WITH DISCRETE LEVEL MODEL)

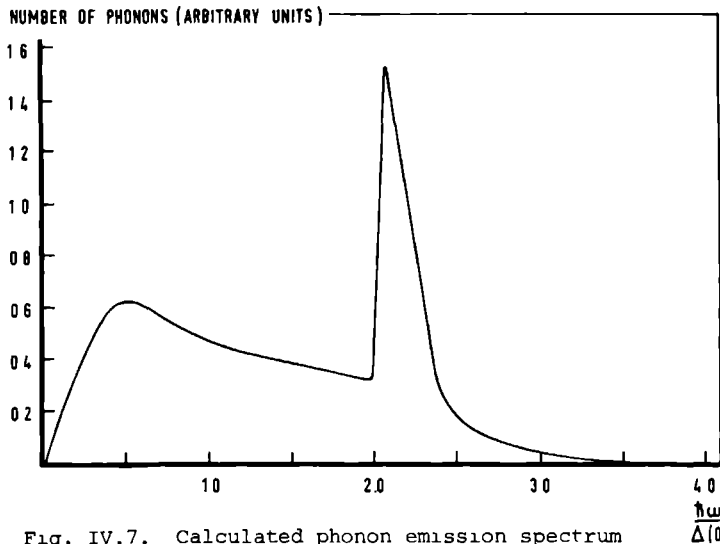


Fig. IV.7. Calculated phonon emission spectrum from a superconductive tunnel junction (after Dayem, Ref. 9). In the discrete level model, 40 energy levels are assumed, spaced at energy intervals of 0.05Δ , up to an energy of 2Δ above the upper gap edge.

quantum of $eV = 2\Delta$, corresponding to the gap-energy. This is a fixed frequency, as it is directly related to the properties of the superconductor, but it can be tuned by an applied parallel magnetic field (H), with $\Delta = \Delta(H)^3$. The recombination linewidth is determined by broadening of the gap-edge by anisotropy and by recombination from adjacent higher energy levels.

The first step relaxation frequency spectrum is continuous in the range $0 < \hbar\omega < eV - 2\Delta$, showing a rather sharp edge at the maximum frequency⁸. By using electronic modulation techniques (differentiation), the effects near the maximum relaxation frequency can be isolated, since the intensity of lower energy phonons is nearly constant. The emitted phonon spectrum has been calculated by Dayem⁹ and is shown in Fig. IV.7 for $eV = 4.0\Delta$. The peak at $\hbar\omega = 2\Delta$ arises from recombination and the broad lower frequency band from relaxation.

When using a set of two symmetrical superconductive tunnel junctions as generator and detector, an effectively 'monochromatic' phonon system centered at the gap-frequency is obtained, as can be seen by folding the spectral distributions of Fig. IV.6 and Fig. IV.7: the generator emits a narrow band at $\hbar\omega = 2\Delta$ and a lower frequency tail, and the detector is sensitive to frequencies $\hbar\omega \geq 2\Delta$ only. The high absorption of phonon energy of $\hbar\omega \geq 2\Delta$ in a superconductor leads to a non-linear buildup of 2Δ -energy phonons with raising injection level at $eV = 4\Delta$. For films thicker than the phonon mean free path, the relaxation phonons of $\hbar\omega \geq 2\Delta$ are re-absorbed within the generator film and provide additional gap-frequency phonons during the de-excitation process. Evidence for the actual occurrence of these processes can be obtained from measurements of the detector signal as a function of generator injection voltage.

The ballistic phonon pulse signal for a setup using symmetric tin-insulator-tin junctions (Sn-I-Sn) on sapphire, as generator and detector of 280 GHz phonons is shown in Fig. IV.8. Impedance matching from the low resistance ($< 1\Omega$) junctions to the 50Ω pulse system is

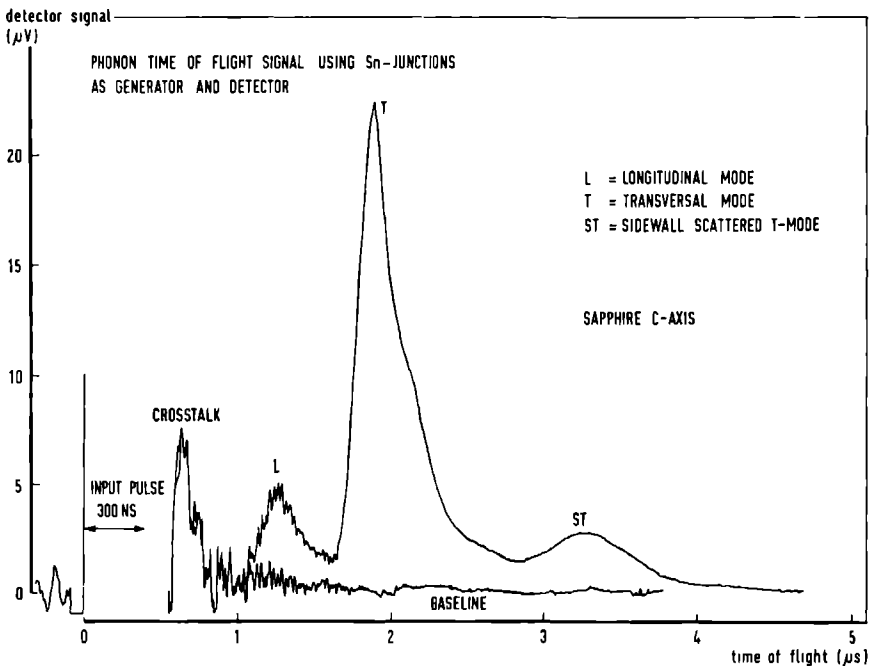


Fig. IV.8 Time-of-flight signal of ballistic phonon pulses in sapphire, using superconductive tunnel junctions as generator and detector of 280 GHz phonons (generator pulse width: 300 nsec, crystal length: 10 mm, crystal diameter: 15 mm).

provided by using a 1Ω impedance stripline and a wide-band 1:7 ratio pulse transformer in both generator and detector circuits, whilst maintaining a 35 nsec risetime. (For a detailed description of the techniques, see sec. III). The recorded (differentiated) phonon signal as a function of generator energy (eV) is plotted in Fig. IV.9. From the current-voltage (I-V) curve (also drawn), the voltage levels corresponding to energies $eV = 2\Delta$, 4Δ , and 6Δ are found. Distinct increases of the signal are detected at these generator energy levels. This provides direct evidence for the narrow-band radiation sensitivity of such a two junction system. For

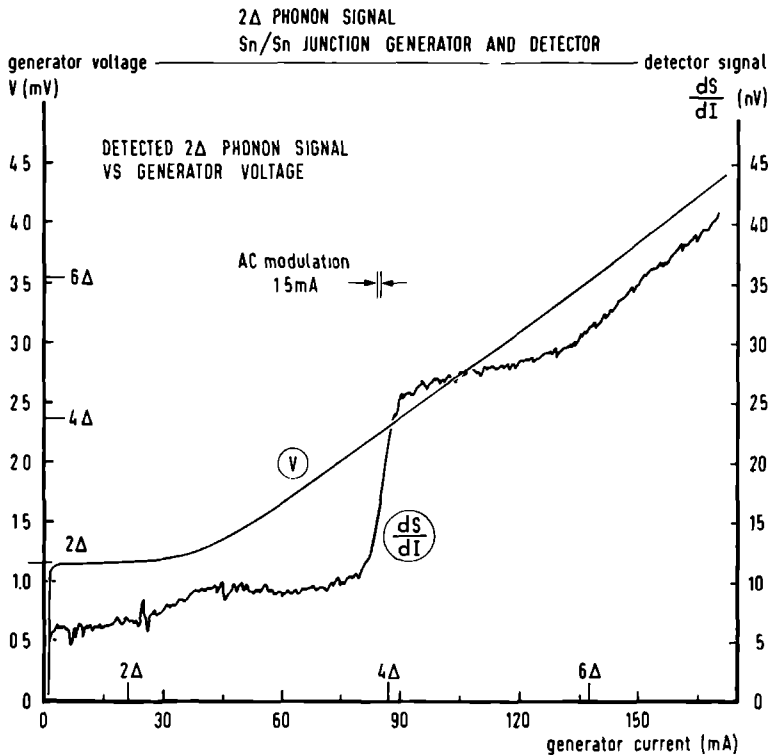


Fig. IV.9 Derivative of received phonon signal as a function of generator energy. The I-V characteristic of the generator junction is also shown. The electronic resolution is indicated by the arrows.

$2\Delta < eV < 4\Delta$, only recombination radiation is detected. The maximum relaxation frequency becomes detectable ($> 2\Delta$) for a generator energy of $eV = 4\Delta$ and the differentiated detector signal increases as this second radiation channel of frequency $\geq 2\Delta$ opens up. The signal increase at $eV = 6\Delta$ demonstrates that re-absorption in the generator is strong and two step relaxation occurs; for a continuing one-step relaxation, no signal increase in the derivative is expected. The weak local maximum at $eV = 2.35\Delta$ reflects the maximum energy level

out of which direct recombination is possible⁹. This indicates a linewidth of 0.35Δ in these experiments. It has been argued that this line broadening is due to the high population injected in levels just above the energy gap in these low impedance junctions. This high-density population tends to spread over a finite energy interval since it is subject to Fermi statistics. The high injection rate is possible only because of the very low tunneling resistance ($10^{-3} \Omega$) and this situation is not reached in higher impedance junctions¹⁰. The results of Fig. IV.9 clearly demonstrate the quantum generation and detection of phonon processes occurring in superconductive tunneling junctions.

REFERENCES

1. A. Dayem and W. Eisenmenger, Phys. Rev. Lett. 18, 125 (1967).
2. W. Eisenmenger, in Tunneling Phenomenon in Solids, edited by E. Burstein and S. Lundqvist (Plenum Press, 1969) p. 371.
3. V. Narayanamurti and R.C. Dynes, Phys. Rev. B6, 143 (1972).
4. H. Kinder, Phys. Rev. Lett. 28, 1564 (1972).
5. J. Schrieffer, in Ref. 2, p. 287.
6. V. Bobetic, Phys. Rev. 136A, 1535 (1964).
7. E. Burstein, D. Langenberg and B. Taylor, Phys. Rev. Lett. 6, 92 (1961).
8. H. Kinder, Z. Phys. 262, 295 (1973).
9. A. Dayem and J. Wiegand, Phys. Rev. B5, 4390 (1972).
10. V. Narayanamurti and R.C. Dynes, Solid State Commun. 12, 341 (1973).

IV.1.3. The acoustic mismatch model

The acoustic mismatch model (AMM) is used to calculate in first approximation the imperfect transfer of phonon energy (heat flow) through the interface of two materials. This may be a solid-solid interface (for instance a metal film deposited onto a dielectric substrate), or a solid-liquid interface. Especially the case of a solid-liquid He-II interface is interesting as the acoustic mismatch is largest here; this situation is generally referred to as the 'Kapitza resistance problem' ¹. In the most basic theoretical approximation, the average energy transmission coefficient is calculated from the acoustic theory of energy transport ^{2,3}. In the simplest case, we assume only longitudinal phonon modes in the two media (1 and 2) forming the interface and also a perpendicular incidence of the energy flux at the interface. From a calculation of the reflection coefficient of a density wave at a boundary surface and using the appropriate boundary conditions, the average transmission coefficient of the acoustic energy from medium 1 to medium 2 (e_{12}) is then given in a straightforward way by:

$$e_{12} = \frac{4z_1 z_2}{(z_1 + z_2)^2} \quad (1)$$

where Z is the acoustic impedance of a medium, which is defined as $Z = \rho c$ (with ρ the density and c the energy group-velocity) ⁴⁻⁶. There is some analogy between the general formulation of the acoustic and electromagnetic energy transfer in interfaces, regarding the role of the respective impedances.

The acoustic impedance of liquid Helium is roughly 10^{-3} times smaller than that of a typical solid, because both the density and the energy velocity are about a factor of 30 lower (see Table III.2.). If we use Eq. (1) for a calculation of the energy transmission coefficient for a solid-liquid He-II interface, then this equation reduces to

$$e_{12} = \frac{4z_2}{z_1} = \frac{4\rho_2 c_2}{\rho_1 c_1} \quad (2).$$

For a sapphire-liquid He-II interface this is calculated to be $3.5 \cdot 10^{-3}$. If we include transmission of phonons, incident at angles θ_1 with the interface-normal, the requirement for conservation of energy and momentum (Snell's law) gives the phonon emission angle θ_2 in the liquid:

$$\frac{\sin\theta_1}{c_1} = \frac{\sin\theta_2}{c_2} \quad (3).$$

When all possible incident angles in the solid are allowed, this leads to a maximum emission angle θ_c in the liquid which is given by

$$\sin\theta_c = \frac{c_2}{c_1} \quad (4).$$

This leads to a critical emission cone with a half-angle of about $3^\circ 7'$. The non-perpendicular incidence also allows the transverse solid modes to excite longitudinal phonons in the liquid Helium.

By combining Eqs. (2) and (4), the transmitted fraction of the total incident energy is found to be:

$$e_{12} \sin^2 \theta_c = \frac{4\rho_2 c_2^3}{\rho_1 c_1^3} \quad (5).$$

This gives a value of about 10^{-4} for a sapphire-liquid Helium-II interface. However, the experimentally found value for this material interface is about 100 times higher.

If we express the energy E of a phonon as $E = \hbar\omega = kT$ (ω : the phonon frequency) the experimentally observed transmission coefficient e_{12} is of the order of 0.1 for phonons with energies equivalent to temperatures T of 1 - 10 K^{8,9}. For low-energy phonons ($T = 0.1$ K), the transmission coefficient approaches the above mentioned AMM limit. It is not too surprising that discrepancies arise at the higher frequencies, since a phonon frequency of $\omega = kT/\hbar = 20 T$ (GHz) implies a wavelength of $500/T$ nm in a typical solid, with T in degrees K.

These high-frequency phonons are scattered increasingly stronger by crystal imperfections (in bulk or in the interface) at higher energies. On the other hand, the acoustic mismatch model seems to be in good agreement with experiments in describing the transmission coefficient averaged over all frequencies in solid-solid interfaces¹⁰, where the same imperfections occur. Also, the anomalous large energy transfer seems to be absent and roughly in accordance with the AMM in cleaved interfaces, as found from recent experiments¹¹.

REFERENCES

1. P.L. Kapitza, J. Phys. (USSR) 4, 181 (1941).
2. W.A. Little, Can. J. Phys. 37, 334 (1959).
3. M.W.P. Strandberg and L.R. Fox, J. Low Temp. Phys. 34, 17 (1979).
4. I.M. Khalatnikov, Zh. Eksp. Teor. Fiz. 22, 687 (1952).
5. G.L. Pollack, Rev. Mod. Phys. 41, 48 (1969).
6. L.J. Challis, J. Phys. C 7, 481 (1974).
7. R.A. Sherlock, A.F.G. Wyatt, N.G. Mills and N.A. Lockerbie, Phys. Rev. Lett. 29, 1299 (1972).
8. C.J. Guo and H.J. Maris, Phys. Rev. A 10, 960 (1974).
9. J.T. Folinsbee and J.P. Harrison, J. Low Temp. Phys. 32, 469 (1978).
10. P. Herth and O. Weis, Z. Angew. Phys. 29, 101 (1970).
11. J. Weber, W. Sandmann, W. Dietsche and H. Kinder, Phys. Rev. Lett. 40, 1469 (1978).

Table IV.2. Table of acoustic properties of sapphire, constantan and aluminium.

		sapphire	constantan	aluminium	units
Debye temperature		980	390	410	K
cutoff frequency	f_{cL}	11.2	9.1	8.8	10^9 Hz
	f_{cT}	9.0	4.6	5.8	10^9 Hz
phase velocity	c_L	11.1	5.24	6.6	10^3 m/s
phase velocity	c_T	6.04	2.64	-	10^3 m/s
density	ρ	3.99	8.8	3.3	10^3 kg/m ³
phonon energy transmission coefficient	e_L	-	0.22	-	
into c-sapphire	e_T	-	0.18	-	

The index L or T refers to longitudinal or transverse phonon modes.

liquid helium ⁴					
pressure		0 bar	24 bar		units
density	ρ	0.14	0.17		10^3 kg/m ³
phase velocity	c	238	360		10^3 m/s

The acoustic impedance of He⁴ increases a factor of 1.8 from 0 to 24 bar.

IV.2.1. Phonon dispersion in He-II

Since many years, the properties of liquid He-II are of considerable interest. From the theoretical point of view, the superfluid He-II phase (resembling a Bose-condensate) is related to superconductivity and He³ superfluidity. Some of the experimental attractions of He-II are: a) it has the isotropic properties of a liquid,

- b) as a liquid, only longitudinal phonons are supported,
- c) it has a high purity (only He³-atoms act as impurities) and it is free of defects,
- d) the dispersion relation $E(k)$ is highly non-linear over a small interval of about 15 K,
- e) the dispersion curve is strongly pressure dependent up to the solidification pressure of 25 bar.

Furthermore it has the unique property of possessing two types of thermal excitations: low-energy phonons (as in pure dielectrics) and rotons with wave-vectors around a minimum energy of 8 K, which occur only in the superfluid. The interaction of these excitations produces the various energy transport modes ("sounds") found in He-II. A detailed knowledge of the transport properties of He-II is also required for a thorough understanding of the problem of energy transfer through solid-liquid He-II interfaces (Kapitza thermal boundary resistance). The He-II elementary excitation diagram $E(k)$, as determined from neutron scattering experiments, is reproduced in Fig. IV.10.

The corresponding regions of the branches are indicated by P for the phonons and R for the rotons. As the density-of-states $D(E)$ of the excitations is inversely proportional to the group velocity $v_g(E) = dE/dk$ at that energy, $D(E) \propto v_g^{-1}(E) = dk/dE$, a high density-of-states is found for maximum energy phonons and minimum energy rotons². For temperatures around $T = 1$ K, the phonon-roton interaction is intense and manifests itself as a collective energy transport mode (second sound)³. For temperatures below $T = 1$ K, this interaction weakens due to thermal de-population (freeze-out) of the high-density roton

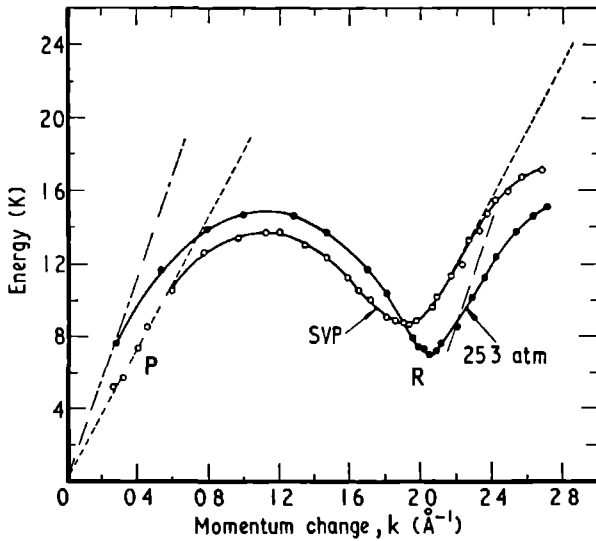


Fig. IV.10. The dispersion curve $E(k)$ for excitations in He-II, as measured by neutron scattering, for He-II pressures of svp and 25.3 bar (after Cowley and Woods, Ref. 1).

levels, at $T < 0.35$ K a liquid with only thermal phonon excitations remains⁴.

An intriguing feature is the existence of an unique anomalous dispersion in He-II under certain pressures⁵. Using the dispersion relation $E(k)$ from Fig. IV.10, the phonon phase velocity is defined as $c_p = E/k$ and the phonon group velocity as $c_g = dE/dk$. In the limit of low frequencies or wavevectors, both velocities converge to the classical sound velocity c_0 . Normal (downward) dispersion, as found in common solid materials, implies $c_p < c_0$ for all energies E . In this case the group velocity $c_g(E)$ is a monotonically decreasing function of the energy E . Anomalous (upward) dispersion, only found in He-II, implies that an energy region exists, where $c_g(E)$ increase above the sound velocity c_0 . If $c_g > c_0$ for low wave vectors (as in

He-II at low pressures), then also $c_p > c_0$. This results in an initial upward curvature of the $E(k)$ diagram for $0.2 \text{ \AA}^{-1} < k < 0.4 \text{ \AA}^{-1}$.

Although the absolute deviations are small (5%), the implications for the allowed phonon scattering processes, are dramatic. Instead of the usual scattering processes, as in a solid, involving 4 phonons (2 in, 2 out), in the region of anomalous dispersion a spontaneous decay of one phonon into two lower-energy phonons is possible. This three phonon process (3PP) thus effectively decreases the mean free path of the phonons with a wavevector in the region where the anomalous dispersion exists. For phonons not involved in the 3PP decay, the normal (long) mean free path ($\text{mfp} > 1 \text{ mm}$) is expected for $T < 0.35 \text{ K}$, as explained above.

The conditions for which the spontaneous decay due to the 3PP occurs, can be found from the $E(k)$ diagram, together with the requirements for conservation of energy and momentum. For a phonon of energy E_1 , excited in He-II at $T = 0 \text{ K}$, where thermal scattering is negligible, we search for the conditions for decay of this phonon into two phonons of lower energy E_2 and E_3 ⁵. Conservation of energy and momentum require

$$E_1 = E_2 + E_3 \quad (1)$$

and
$$\vec{p}_1 = \vec{p}_2 + \vec{p}_3, \quad (2)$$

from which follows the inequality:

$$|p_1| \leq |p_2| + |p_3| \quad (3)$$

It is easy to see that for a sonic wave $E = c_0 p$ both (1) and (2) can be satisfied, and all three phonons are collinear: there is no scattering over small angles. If we extend the situation to phonons with different velocities depending on energy (resp. c_1 , c_2 and c_3), as in the realistic liquid, we get from (1):

$$c_1 p_1 = c_2 p_2 + c_3 p_3 \quad (4)$$

and this can be rewritten to:

$$P_1 = \left(\frac{c_2}{c_1}\right)P_2 + \left(\frac{c_3}{c_1}\right)P_3 = P_2 + P_3 + \left(\frac{c_2-c_1}{c_1}\right)P_2 + \left(\frac{c_3-c_1}{c_1}\right)P_3 \quad (5)$$

If the velocities of the decay phonons are larger than the initial phonon velocity ($c_2 > c_1$ and $c_3 > c_1$) we find from Eq. (5) that $P_1 > P_2 + P_3$ and hence momentum cannot be conserved (Eq. (3)). This implies that for normal dispersion (continuous decreasing $c_g(E)$) this spontaneous decay cannot occur and a phonon of energy E_1 has a very long lifetime. This occurs in He-II for pressures $p > 18$ bar. In the case that the velocities of the decay phonons are both smaller than the initial phonon velocity ($c_2 < c_1$ and $c_3 < c_1$) the last two terms in Eq. (5) are negative, and this equation is consistent with the momentum conservation requirement. These criteria ($c_2 < c_1$ and $c_3 < c_1$) can be fulfilled at low He-II pressures ($p < 10$ bar) due to the initial upward dispersion $c_g(E) > c_0$. Spontaneous decay of a phonon of energy E_1 between 2K and 6K will result⁵.

The energy interval where this 3PP is in operation moves to lower wavevectors with increasing pressure, and for $p > 18$ bar a normal dispersion is found⁶.

The possibility of this spontaneous decay was suggested by Feynman⁷. After additional analysis⁸ and early pulse experiments to detect this phenomenon⁹, clear evidence was found in specific heat measurements¹⁰. It was also indicated by neutron scattering data¹. Agreement between ultrasonic absorption results¹¹ and theory was found by Maris and Massey¹², introducing explicitly an upward dispersion. From re-analysis of ultrasonic data, Jackle and Kehr could estimate the cutoff energies for the 3PP⁶. Small angle phonon scattering was observed in heat pulse experiments in liquid He-II¹³. The most convincing results are found in the work of Narayanamurti and Dynes, who measured the phonon group velocity at 90 GHz and obtained directly the cutoff energies for the 3PP as a function of He-II pressure¹⁴.

IV.2.2. Ballistic phonon pulses in He-II at $T < 0.35$ K

Pure ballistic phonon transport in liquid He-II expected for temperatures $T < 0.35$ K where the liquid contains only thermal phonon excitations. Phonon energy transport is then analogous to that in high-quality dielectric single crystals in the thermal boundary scattering regime, where the phonon mean free path is limited by sample dimensions only. In our experiment, fast thin-film thermal transducers¹⁵ are mounted opposite each other in a teflon cell with large lateral dimensions, delaying sidewall reflections sufficiently as not to interfere the direct signal (see sec. III.1 and Fig. III.2). This assembly is mounted on the detachable flange of a pressure chamber which is filled with He-II and cooled to $T = 0.080$ K by means of a dilution refrigerator (sec. III.3).

The length of the He-II cell is accurately calibrated to be 2.44 ± 0.02 mm by measuring the time interval between successive second sound pulses at $T = 1.7$ K and using the well documented data on second sound velocity¹⁶. When using low generator power densities, excellent ballistic pulse signals are observed. (Fig. IV.11). The

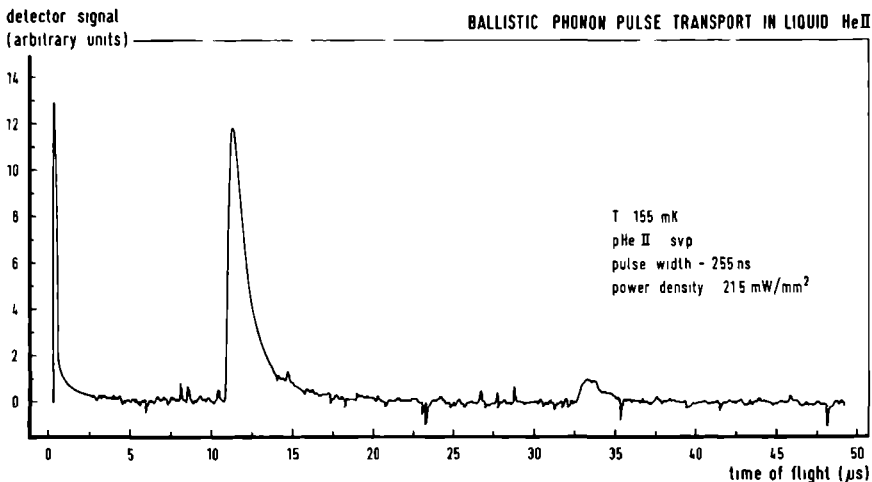


Fig. IV.11. Ballistic phonon pulse signal in liquid He-II. For experimental conditions see figure. A three transit echo is seen at 32.5 μ sec.

calculated black-body heater temperature is $T_h = 3.2$ K, however due to the large acoustic mismatch between the solid film and liquid He-II, the actual frequency distribution in the liquid may be rather different from the one corresponding to this temperature (see sec. IV.3.3).

The pulse arrival velocity is plotted as a function of the He-II sample temperature in Fig. IV. 12b. For $T < 0.35$ K, the signal arrival time is no longer delayed by thermal scattering processes, and the ballistic regime is reached. These data were taken with a fixed (persistent) magnetic field on the detector.

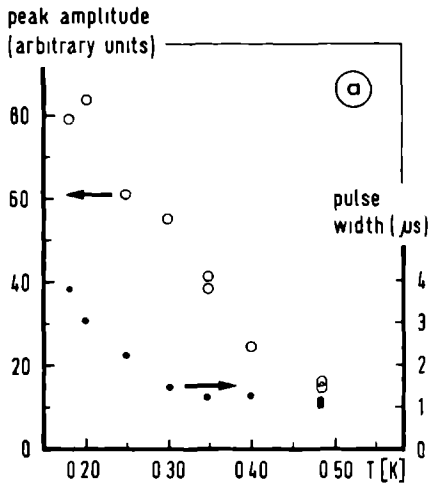


Fig. IV.12a. Phonon signal intensity and pulse width as a function of He-II sample temperature.

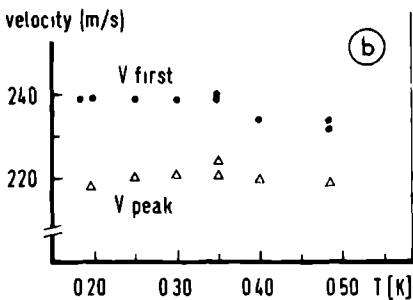


Fig. IV.12b. Signal arrival and peak velocity as a function of He-II temperature. Experimental conditions for Fig. IV.12a and b: He-II pressure: 1.2 bar, pulse width: 300 nsec, power density: 23 mW/mm², He-II cell length: 2.44 mm.

The increase of signal amplitude (Fig. IV.12a) at low temperatures has two origins: the main increase is due to decreased scattering by thermal phonons in the liquid, the other is the small change (about 10%) in detector sensitivity, optimized at $T = 0.15$ K; similar arguments can be used for the signal pulse width. The changing detector sensitivity is due to the slight decrease in T/T_c for the superconductive Al detector in the fixed magnetic field; this changes the bias point at the resistive transition of the film in the magnetic field. The signal intensity at fixed temperature was increasing linearly with the detector bias current in the range of 10-120 μ A. The energy dissipation in the detector was always below 0.1 μ W; the generator power density was kept below 30 mW/mm², corresponding to an energy of 10^{-8} J/mm² per pulse. For power densities above 50 mW/mm², non-linearities in the pulse signal were observed. From Fig. IV.12b it can be noted that the signal peak velocity is not noticeably temperature dependent for $T < 0.5$ K; the signal arrival velocity, corresponding to the phonons propagating in a direct line from generator to detector, reaches a constant value of 238 ± 3 m/s below $T = 0.35$ K. If we assume that the phonons in the peak of the signal also have this velocity but are scattered over small angles, we find that their scattering angle is 13 ± 2 degrees at a pressure of $p = 1.2$ bar. For temperatures above $T = 0.7$ K, the well-known pulsed second sound signals are observed¹⁷.

The influence of the He-II hydrostatic pressure on the signal intensity, pulse arrival and peak velocity is shown in Fig. IV.13. For saturated vapour pressure (svp) the signal arrival velocity is, within the experimental error, in agreement with the low frequency sound velocity of 238 m/sec, determined at 105 MHz¹¹. The calibration of the propagation path was made using the well-known second sound velocity at higher temperatures; a He-II cell length of 2.44 ± 0.02 mm is found. However, at a pressure of 24 bar the measured arrival velocity is substantially lower than the velocity of 360 m/sec¹⁸, found from ultrasonic data. This result is not understood at present.

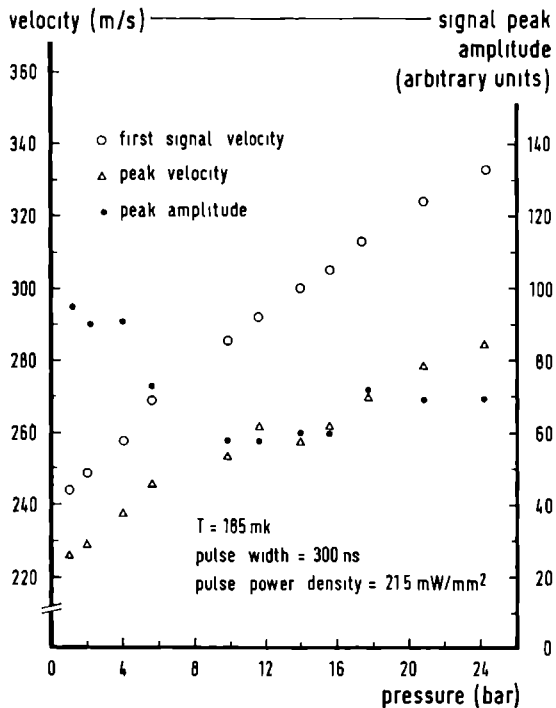


Fig. IV.13. Phonon signal intensity, pulse arrival and peak velocity as a function of He-II pressure. For experimental conditions, see figure.

As can be seen from Fig. IV.13, the signal peak amplitude does not vary much with the He-II pressure above $p = 8$ bar. Due to the existence of the spontaneous 3PP decay and the resulting scattering over larger angles in He-II at low pressures, a decrease in signal intensity on lowering the He-II pressure is expected for the phonons which have a group velocity $v_g(E)$ larger than c_0 (see sec. IV.2.1). If a phonon frequency distribution corresponding to the calculated heater temperature of $T = 3.2$ K is emitted from the heater into He-II then, due to the radiation bandwidth $\Delta E = 2.8 kT_h$, a large part of

the phonon flux in the liquid is subject to the 3PP decay at this low pressure. From this and other evidence¹⁹ it is suggested that the phonon distribution propagating in He-II has a lower pulse temperature, although the calculated heater temperature is correct (see also sec. IV.3.3). The pulse temperature in the liquid is then estimated to be a factor of 2 lower than the one calculated from the power density¹⁹. For the pulse temperature found in this way, the dispersion curve just begins to show a noticeable upward curvature, and no strong 3PP is present for the phonon frequency involved. For these low energies, the group and phase velocity of the phonons do not differ much from the sound velocity, and collinear scattering is allowed⁵.

The pressure dependence of the velocity cannot be understood in this model. In this respect, it should be very much worthwhile to work backwards from the received velocity profiles in order to obtain the involved frequency distributions, with a deconvolution scheme as suggested in Refs. 19 and 20, using explicitly the group velocity $v_g(E)$ for all energies.

REFERENCES

1. A.D.B. Woods and R.A. Cowley, Rep. Mod. Phys. 36, 1135 (1973).
2. R.C. Dynes and V. Narayanamurti, proceedings of the EPS topical conference on liquid and solid Helium, July 1974, Haifa (edited by C. Kuper, S. Lipson and M. Revzon), J. Wiley, New York and Israel University press.
3. I.M. Khalatnikov, Introduction to the theory of superfluidity, Benjamin, New York (1965).
4. R.W. Guernsey, Jr., Ph.D. thesis, Washington University, St. Louis, 1968, unpublished.
5. H.J. Maris, Rev. Mod. Phys. 49, 341 (1977).
6. J. Jäckle and K.W. Kehr, Phys. Rev. Lett. 27, 654 (1971).
7. R.P. Feynman, Phys. Rev. 94, 262 (1954).

8. H.W. Jackson and E. Feenberg, Rev. Mod. Phys. 34, 686 (1962).
9. R.W. Guernsey and K. Luszczynski, Phys. Rev. A3, 1052 (1971).
10. N.E. Phillips, C.G. Waterfield and J.K. Hoffer, Phys. Rev. Lett. 25, 1260 (1970).
11. P.R. Roach, J.B. Ketterson and M. Kurchnir, Phys. Rev. Lett. 25, 1002 (1970).
12. H.J. Maris and W.E. Massey, Phys. Rev. Lett. 25, 220 (1970).
13. N.G. Mills, R.A. Sherlock and A.F.G. Wyatt, Phys. Rev. Lett. 32, 978 (1974).
14. R.C. Dynes and V. Narayanamurti, Phys. Rev. B12, 1720 (1975).
15. R.J. von Gutfeld and A. Nethercot Jr., Phys. Rev. Lett. 12, 641 (1964).
16. J. Maynard, Phys. Rev. B14, 3868 (1976).
17. R.W. Guernsey Jr., K. Luszczynski and W. Mitchell, Cryogenics, 110, april 1967.
18. R.C. Dynes, V. Narayanamurti and K. Andres, Phys. Rev. Lett. 30, 1129 (1973).
19. R.A. Sherlock, A.F.G. Wyatt and N.A. Lockerbie, J. Phys. C10, 2567 (1977).
20. M.P.W. Strandberg and L.R. Fox, Phys. Lett. 62 A, 151 (1977).

IV.2.3. Shock wave generation in He⁴ gas at T = 1.2 K.

Using an experimental setup of two oppositely mounted pulse transducers (Fig.III.2) , as described in sec.III.1, a superfluid He-II film will cover all walls of the cell for temperatures $T < 2.17$ K, when enough He⁴ gas is condensed to form a small puddle of liquid. Upon applying short current pulses to the heater film, part of the superfluid film will evaporate and some of the evaporated He⁴ atoms propagate as a pressure wave to the detector film, where a short temperature transient results at the impingement. The He⁴ gas pressure is 1.5 to 5.0 torr. Analysis of the shockwave signals provides data on the sound velocity in He⁴ gas and on the thickness and creep speed of the superfluid He-II film. For a liquid level above the transducer films, the well-known second sound pulses in He-II are observed.

SHOCK WAVE GENERATION IN HELIUM GAS BY FAST EVAPORATION OF A SUPERFLUID HELIUM FILM

J W M BAKKER, H Van KEMPEN, H W M SALFMINK and P WYDER

Physics Laboratory, University of Nijmegen, The Netherlands

Received 12 October 1972

The generation and detection of shock waves in cold helium gas by means of exploding superfluid helium films and superconducting tunnel junctions is described. The method can also be used to study the properties of superfluid films.

We have generated shock waves in helium gas by fast evaporation of the superfluid film covering a heater. The heater consisted of a constantan film of about 50 Ω resistance evaporated onto a glass slide. The shock waves were generated by driving the heater with current pulses of 260 nsec duration. The dissipated energy evaporates the helium film partly or fully depending on the energy I of the pulse. The fast bolometer detector consisted of a tin-tin superconducting tunnel junction as described by Esernenger and Dayem [1]. The substrates of the generator and the detector were in contact with the pumped helium bath ($p = 0.5$ torr, $T = 1.2$ K) via copper braids. Experiments with second sound pulses in liquid helium using this system showed that there is a linear relation between the square root of the pulse energy \sqrt{I} and the detector signal voltage V_d .

We wish to report three series of measurements (indicated by I, II and III) with three different generators and detectors. In I (the generator and detector substrates were vertical with a fixed distance of 1.35 mm in II and III the substrates were horizontal and the distance could be remotely controlled).

Fig. 1A shows the detector signal as a function of \sqrt{I} . At an energy of 7.6×10^{-8} joule there is a sharp break in the curve of series I. This can be interpreted as the energy which is just sufficient to evaporate the entire helium film. The thickness of the film can be calculated from this energy and from the area of the heater assuming that the heat of evaporation of the film is the same as that of the bulk liquid. It is found to be 240 Å. This is of course an upper limit because not all the energy is necessarily dissipated in the film, yet this value agrees very well with the thicknesses

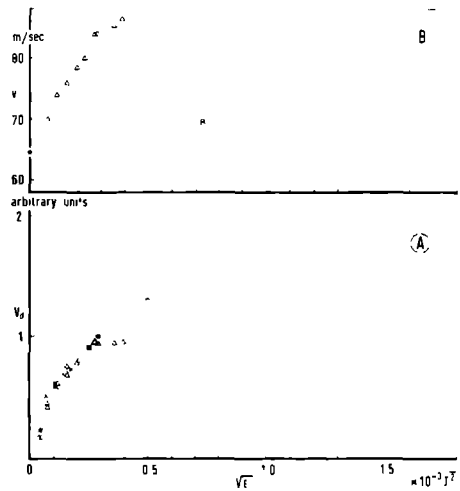


Fig. 1. A) Detector signal V_d versus the square root of the generator energy \sqrt{I} . Δ series I, \times series II, \circ series III. The signals V_d are scaled in such a way that all three series go through the point indicated by +. B) Velocity of the shock wave versus square root of the generator energy \sqrt{I} . Δ series I, \times series II, \circ series III. The calculated sound velocity for an ideal gas is indicated by \bullet .

found for vertical helium films in other experiments [e.g. 2]. For the horizontal arrangement of series II and III, the break in the V_d versus \sqrt{I} curve is not so clear.

Fig. 1B gives the observed velocity of the shock

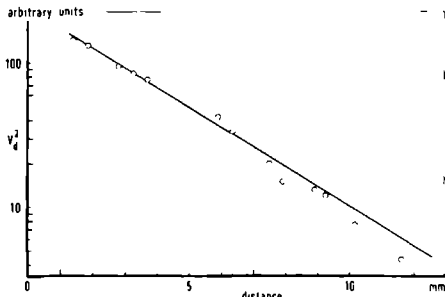


Fig. 2. Square of detector signal voltage V_d^2 versus distance between generator and detector.

waves versus \sqrt{E} for series I and III. One notes the increasing velocity as a function of energy, which is typical for shock waves. For energies approaching zero the velocity should be the usual sound velocity. It is seen that the velocity approaches 62 m/sec and 58 m/sec for I and III respectively. This difference in extrapolated values can be due to the errors in the distance determination ($1.35 \text{ mm} \pm 6\%$ for I, $1.85 \text{ mm} \pm 3\%$ for III). The calculated sound velocity (assuming ideal gas behaviour) for helium gas is also indicated in fig. 2. Remarkably, the rise in velocity is much steeper in I than in III. It is not yet clear whether this is due to a thicker helium film present in series III (as suggested by fig. 1A) or to the different geometry of the two arrangements. Further research is in progress on this matter.

Fig. 2 shows the detector signal as a function of the distance between generator and detector. There are two mechanisms which contribute to the decrease of

signal with distance: attenuation of the shock wave as a result of the energy dissipation in the shock front and spreading of the wave front. In order to separate these two contributions, measurements of the angular dependence of the energy of the shock wave are in progress. The exponential dependence on distance as indicated in fig. 2 suggests a strong collimation of the shock wave.

For the measurements of figs. 1 and 2 we used a repetition frequency of 100 Hz. For very high repetition frequencies the helium film will not be able to cover the whole heater area again during the time between the pulses. Thus for increasing repetition frequencies a limit will be reached above which the detector signal will decrease. From this limit and from the dimensions of the heater, the recovery speed of the film can be determined. Preliminary measurements on I with $E = 7.6 \times 10^{-8}$ joule and on II with $E = 1.9 \times 10^{-8}$ joule gave a recovery speed of 39 cm/sec and 8.1 cm/sec respectively, which is of the same order of magnitude as found [2] for the film creep speed (30 cm/sec) at this temperature.

In the present experiment we were not yet able to verify whether the pressure wave had the shape characteristic for shock waves because the transformer, matching the detector to the preamplifier, distorted the signal. It might be useful to attempt pressure sensitive detection together with temperature sensitive detection in future experiments.

References

[1] W. F. Fritsmenger and A. H. Dayem, Phys. Rev. Letters 18 (1967) 125.
 [2] J. Wilks, The properties of liquid and solid helium (Clarendon Press, Oxford, 1967).

IV.3. TRANSMISSION OF BALLISTIC PHONON PULSES THROUGH A SAPPHIRE-LIQUID He-II INTERFACE.

This section contains the results of experiments with ballistic phonon propagation through sapphire-liquid He-II interfaces, in an attempt to provide an alternative technique for investigation of the Kapitza thermal boundary resistance. Knowledge of the phonon propagation characteristics of the two materials under study (sapphire and superfluid He-II) is required for an interpretation of these experiments. These properties are partly found from experiments described in sec.IV.1 on sapphire, in sec.IV.2 on liquid He-II and from the extensive literature (see the references of sec.IV.3.3). Preliminary results are given in sec.IV.3.1. The most important experimental findings are given in sec.IV.3.2, and a more extensive analysis is presented in sec.IV.3.3.

TRANSMISSION OF BALLISTIC LONGITUDINAL AND TRANSVERSAL PHONON PULSES THROUGH A SAPHIRE-HeII INTERFACE AT $T = 0.25$ K

H W M. Salemink, H. van Kempen and P. Wider

Research Institute of Materials, University of Nijmegen, Toernooiveld, Nijmegen, The Netherlands

Resumé.- En employant des techniques de "heat-pulse" rapides, nous avons observe la transmission de phonons balistiques longitudinaux (L) et transversaux (T) du saphir aux phonons dans l'hélium superfluide à une température de $T = 0,23$ K. Le rapport d'intensité des modes L et T converties était de $0,22 \pm 0,02$, tandis qu'une valeur de $0,31 \pm 0,01$ pour cette même grandeur a été observée dans le saphir.

Abstract - Using fast heat-pulse techniques, the transmission of ballistic longitudinal (L) and transversal (T) phonons from sapphire into phonon in superfluid He-II at $T = 0.23$ K has been observed. The intensity ratio of the converted L and T mode in He-II was found to be 0.22 ± 0.02 whereas a value of 0.31 ± 0.01 was obtained for the sapphire crystal

The transmission probability of phonons from solids to liquid He still raises many questions both theoretically as experimentally. To gain more insight one has tried to study the transmission of longitudinal (L) and transversal (T) phonons separately by means of time-of-flight techniques. Up to now in most experiments the reflection from the surface under study has been measured [1]. However, among others because of the presence of phonon focusing, the interpretation of the reflection experiments is not straight forward, so direct transmission experiments are preferable [2].

In this paper experiments are described on transmission of ballistic phonon pulses from single crystal sapphire to superfluid He-II at environmental temperatures below 0.25 K and under hydrostatic pressures up to 25 bar. Under these conditions phonon transport in He-II is purely ballistic [3]. Time-of-flight techniques are used to resolve the phonon pulses in He-II, originating from longitudinal (L) and transverse (T) mode phonons in the sapphire crystal. Since the converted phonon pulses in He-II propagate under identical conditions, the conversion of L and T mode phonons at the solid-liquid-interface can be studied, thus providing a new technique for investigation of the Kapitza resistance.

The experimental arrangement is shown in figure 1. A high time resolution has been obtained by using thin film transducers. Heat pulses are generated into the source material (single crystal sapphire, along c-axis) by an evaporated thin film

heater

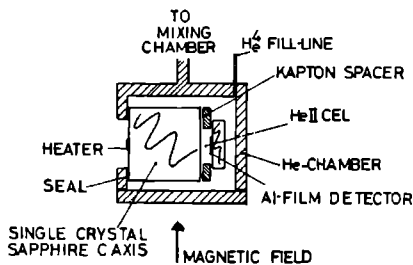


Fig. 1 Experimental arrangement.

The heater is backed by a vacuum to ensure that all energy is directed into the crystal. After passing through the sapphire-He interface, the converted phonon pulses are detected by a superconductive Al-film bolometer in the superfluid, placed at a distance of 0.5 mm from the sapphire surface under study. The whole assembly is mounted in a pressure cell and cooled to $T < 0.25$ K by means of a dilution refrigerator. The space between the detector and the sapphire surface is filled with high-purity liquid helium under pressures of up to 25 bar.

A typical detected time-of-flight signal at a temperature of $T = 0.22$ K and a He-II pressure of 24 bar is shown in figure 2. Distinct phonon pulses are seen, whose arrival times coincide well with the expected transit times for converted L, T

and sidewall reflected (SW) pulses as well as echo's from these pulses in the He-II cell (L3,f3).

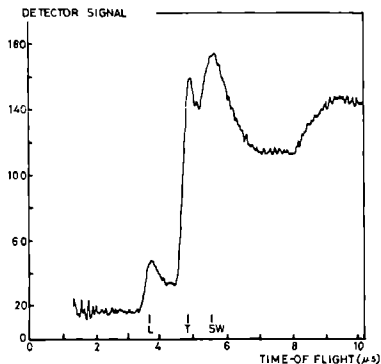


Fig. 2 : Time-of-flight signal. $T = 0.22$ K, $p = 24$ bar. Vertical scale in arbitrary units.

The peak signal intensity of the converted L and T phonon modes, detected in He-II, as a function of the heater power density is shown in figure 3.

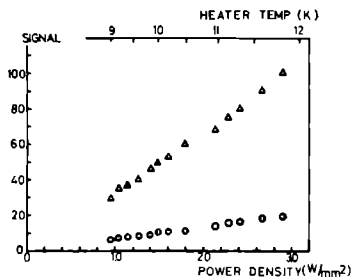


Fig. 3 . Signal peak intensity vs. heater power density. Vertical scale in arbitrary units, circles L mode, triangles T mode $T = 0.23$ K, $p = 24.8$ bar.

The indicated heater temperatures are calculated from the input power density /4/. The measured ratio of the converted L and T mode signals is 0.22 ± 0.02 over the input power density range of 1 to $3W/mm^2$, whilst a value of 0.31 ± 0.01 is found for the L/T ratio in the sapphire itself. This is in contrast with the results of transmission experi-

ments, using second sound excitations at 1.5 K, where no change in the converted L/T intensity ratio relative to the ratio in the solid was observed /5/.

Upon reduction of the He-II pressure the converted L and T mode signals decrease in intensity, with a large step around $p = 14$ bar. The converted L/T ratio decreases too, leading to a value of 0.15 ± 0.02 at $p = 1$ bar. On the basis of the acoustic mismatch theory and its modifications, the observed values and the shifts in the detected L/T ratio is unexpected. However, an explanation can be attempted taking into account the broad energy spectrum of the phonons involved. Experiments with monochromatic phonons should certainly be very useful to unravel this problem.

Part of this work has been supported by the "Stichting voor Fundamenteel Onderzoek der Materie" (FOM) with financial support from the "Nederlandse Organisatie voor Zuiver Wetenschappelijk Onderzoek" (ZWO).

References

- /1/ Guo, C -J., Maris, H.J., Phys. Rev. 10(1974)960
- /2/ Taylor, B., Maris, H.J., Elbaum, C., Phys. Rev. B3 (1971) 1462
- /3/ Narayanamurti, V., Dynes, R.C., Andres, K., Phys. Rev. B11 (1975) 2500
- /4/ Weiss, O., Z. Angew. Phys. 26 (1969) 325
- /5/ Swanenburg, T. J.B., Wolter, J., Phys. Rev. Lett. 31 (1973) 693
- /6/ Khalatnikov, I. M., An introduction to the theory of superfluidity (N.Y., Benjamin 1965)

Ballistic-Phonon-Pulse Transmission through a Solid-Liquid He II Interface at $T=0.25$ K

H W M Salemink, H van Kempen, and P Wyder

*Physics Laboratory and Research Institute for Materials, University of Nijmegen, Toernooiveld Nijmegen
The Netherlands*

(Received 10 July 1978)

The transmission of ballistic longitudinal (L) and transverse (T) phonon pulses from sapphire to liquid He II at temperatures of $T = 0.25$ K has been measured as a function of the pulse power and He II hydrostatic pressure for the first time. Under these experimental conditions, the converted L- and T-mode pulses propagate ballistically through He II. The results indicate that the transmission probability is different for the L and T modes and that the intensity ratio of converted L and T modes changes with the He II pressure.

The transmission of phonon energy through solid He II interfaces has attracted a great deal of theoretical and experimental interest in recent years.^{1,2} Despite many very interesting findings³ and the use of new phonon-pulse techniques,⁴ the problem still evades solution. Because of the existence of phonon focusing in anisotropic solids,⁵ the interpretation of the more simple and most common reflection experiments is not unambiguous⁶ and energy-transmission experiments are needed. However, in the phonon-pulse transmission experiments performed up to now, either the time resolution was too low to resolve converted longitudinal (L) and transverse (T) modes,⁷ or the temperature of He II was so high ($T \approx 1.5$ K) that the phonon-roton interaction was intense and the energy transport from the interface oc-

curred in a collective mode (second sound) resulting in a very small phonon mean free path.⁸ In this paper, we report on the first observation of the direct conversion of L- and T-polarized phonon pulses from a solid into well-resolved ballistic-phonon pulses in liquid He II. The experimental conditions (He II temperature $T = 0.23$ K, hydrostatic pressure $p = 24$ bar) are such that, as a result of the normal (downward) dispersion relation of He II, the phonon mean free path l in He II is macroscopic ($l > 1$ mm).⁹ The conversion of L and T phonon modes at the solid-liquid interface can therefore be studied in a direct way.

In the present experiment, fast-heat-pulse techniques at very low temperatures are used for the time resolution of the converted L and T modes. Our measurements indicate a changed ratio of

the pulse intensities (L-mode pulse intensity divided by T-mode pulse intensity, L/T ratio) in the liquid, after conversion at the interface, as compared with this ratio in the solid crystal. The individual converted L- and T-mode pulses have different dependences on the heater temperature, and the L/T ratio of the converted L and T modes decreases on lowering the He II hydrostatic pressure.

The experimental arrangement is shown in the inset of Fig. 1. An evaporated-thin-film heater (H) (1-mm^2 area) is used to generate ballistic phonon pulses in a single-crystal sapphire (C), the propagation direction is chosen to be parallel to the c axis where the T mode is degenerated. The heater is backed by a high vacuum (VC), therefore all the phonon energy is directed into the crystal. After conversion of the modes at the interface the resulting ballistic phonon pulses in He II are detected by a superconducting aluminum thin-film bolometer (D), evaporated on a sapphire substrate and current biased at the

resistive transition in a parallel magnetic field. The detected signals are linear with the bias current in the range used (up to $100\ \mu\text{A}$). The propagation length in He II of $0.59\ \text{mm}$ has been measured accurately with second-sound reflections at $T = 1.5\ \text{K}$. The whole assembly is mounted in a pressure chamber (PC) and cooled to a temperature of $T = 0.20\ \text{K}$ by means of a dilution refrigerator (DR). The He II chamber is filled (f) with high-purity ^4He and can be pressurized up to $p = 25\ \text{bar}$. Short current pulses ($150\ \text{nsec}$) are used on the generator and detection is accomplished by means of a time-of-flight technique using a Biomation 8100 transient recorder (10-nsec resolution) and a digital signal averager.

A typical time-of-flight signal is shown in Fig. 1. The arrival times coincide within experimental accuracy ($50\ \text{nsec}$) with calculated values using sound-velocity data and crystal-transient times. It should be noted that the signals are all longitudinal phonon pulses in liquid helium but that they originate from the conversion of longitudinal and transverse phonons in the sapphire. Figure 2 shows the peak-height values of converted L and T modes as a function of the pulse power at the generator. The heater temperature indicated in Fig. 2 is derived from the power den-

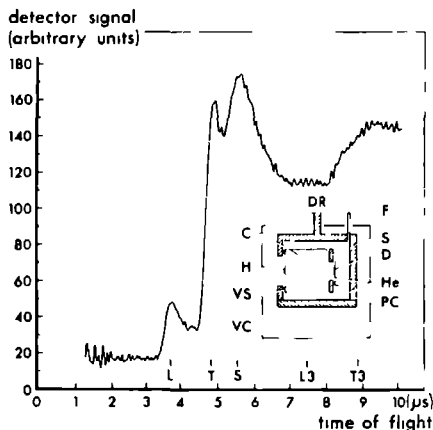


FIG. 1. Detected time-of-flight signal. L, T, and S refer to longitudinal phonons in liquid He II, originating from longitudinal, transverse, and sidewall-reflected phonon modes in the sapphire crystal. L3 and T3 indicate the expected flight times for three transit echos in the He II cell (He II temperature $T = 0.20\ \text{K}$, He II pressure $p = 24\ \text{bar}$, pulse power density $1.48\ \text{W}/\text{mm}^2$). The inset shows the experimental assembly: DR, dilution refrigerator; F, ^4He fill line; S, Kapton spacer; D, aluminum film detector; He, liquid He II; PC, pressure chamber; VC, vacuum chamber; VS, vacuum seal; H, thin-film heater; C, single-crystal sapphire.

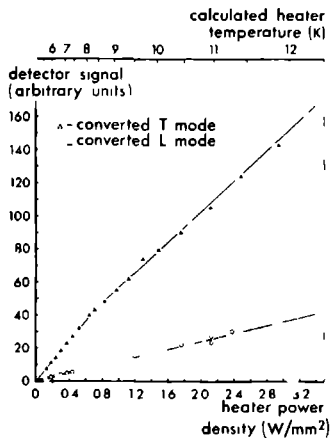


FIG. 2. Intensity of converted L and T modes as a function of heater power density. The indicated heater temperature is calculated with the assumption of a black-body phonon radiation (Environmental He II temperature $T = 0.23\ \text{K}$, He II pressure $p = 24\ \text{bar}$, pulse width $150\ \text{nsec}$).

sity of the generator using Weis's¹⁰ calculations of black-body phonon radiation. Figure 2 shows that, within experimental accuracy, the converted L mode has one single linear power relation, whereas the converted T mode has two regimes of linear dependence, changing slope at 0.8 W/mm^2 . The power density of this breaking point corresponds to a calculated heater temperature of 8.3 K , somewhat higher than the estimated minimum roton energy¹¹ at $T = 0.20 \text{ K}$ and $p = 24 \text{ bar}$ ($\sim 7.5 \text{ K}$). Nonlinear detector operation can be ruled out as we have checked the linearity of the signal as a function of the pulse energy, resulting in signal levels of about 3.5 times the maximum shown in Fig. 2. A second point to be mentioned is the measured intensity ratio of the converted L and T modes which is 0.20 ± 0.02 below 0.8 W/mm^2 and increases to 0.24 ± 0.02 for power levels above 0.8 W/mm^2 . The analogous L/T-mode intensity ratio found in the sapphire crystal itself using identical geometries for generator and detector films is found to be 0.31 ± 0.01 , in close agreement with theoretical calculations¹² predicting a ratio of 0.33. This result is in contrast with transmission measurements using second-sound excitation at $T = 1.5 \text{ K}$ where the L/T ratios were found to be equal in the solid and in the liquid.⁸ Our measurements indicate an enhanced transmission for T-mode phonons relative to the L mode. Qualitatively the same conclusion follows from the results of Guo and Maris,⁶ who found a smaller reflection coefficient for T- than for L-mode phonons from a solid to He II. Both these findings are in contrast with the recent results of Weber, Sandermann, Dietzsche, and Kinder⁷ from a reflection experiment where definite clean surfaces were used.

In Fig. 3(a) the amplitudes of the converted L and T modes are shown as a function of the hydrostatic He II pressure. The large decrease of the signals for lower pressures is due to the onset of anomalous dispersion at $p < 14 \text{ bar}$ as has been seen in transmission experiments through bulk He II.^{13,14} However, the influence of pressure is not equal on both modes [Fig. 3(b)], the converted L/T ratio shifts from 0.22 ± 0.02 at $p = 24 \text{ bar}$ to 0.13 ± 0.02 at $p = 1 \text{ bar}$. We can imagine two possible explanations for this shift. First, it is possible that the influence of pressure on the conversion at the interface is different for the L or the T mode, however, this mechanism is expected to exhibit a monotonic behavior as a function of He II pressure with no drastic changes around $p = 14 \text{ bar}$ [Fig. 3(a)]. The second ex-

planation is based on the broad phonon frequency distributions involved in these experiments. The detected signal ratio is not expected to change over the whole pressure range ($1\text{--}25 \text{ bar}$) during propagation through (isotropic) He II if both converted modes have identical frequency distributions. Therefore the shift in detected ratio with He II pressure can be interpreted as an indication of different frequency distributions (unequal pulse temperatures) in the transmitted phonon modes. Our results indicate that the L mode is more effectively down-converted in frequency than the T mode. This implies that the indicated heater temperature (Fig. 2) cannot be identified with the pulse-temperature in He II. Other phonon experiments¹⁵ have also indicated that a substantial discrepancy exists between calculated heater temperatures and the observed effective pulse temperatures in He II. Application of these results scales down our effective pulse tempera-

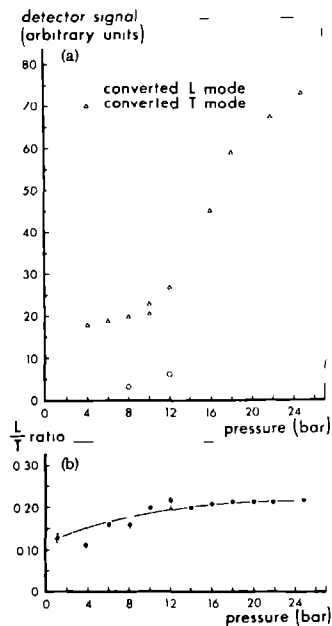


FIG. 3 (a) Intensity of converted L- and T-mode signals as a function of He II pressure. (b) Converted L/T-mode intensity ratio as a function of He II pressure. $T = 0.23 \text{ K}$, pulse width 150 nsec , pulse power density 1.56 W/mm^2 .

tures in He II with a factor of about 3.5 at a power level of 1.0 W mm^2 .

Following the same reasoning, one might be tempted to argue that the change in slope in the converted T mode at 0.8 W mm^2 (Fig. 2) could be related to the minimum energy ($\sim 8 \text{ K}$) for direct coupling the phonon flux to roton excitations in He II. Because of the black-body radiation involved, the effect of the 8-K energy levels is expected to show up at frequencies $\omega = 2.8kT/\hbar$, where T is the effective pulse temperature. Taking into account the above mentioned scaling down of the temperatures, the break in slope appears at approximately the right energy for direct roton excitation. However, the rather sharp break in slope is not to be expected on the basis of a broad Planck distribution.

The results from our phonon-transmission experiments show clearly a changed L/T ratio found after propagation through the interface, as compared with this ratio in the solid crystal. The observed pressure dependence indicates that during conversion the frequency distribution (effective pulse temperature) of the L-mode phonon pulse is more strongly affected than that of the T-mode phonon pulse. Obviously, these first experiments should be refined with use of tunnel junctions as quasimonochromatic phonon generators and detectors and by better surface characterization.

We are most grateful to Dr. J. Wolter for interesting discussions on this subject. Part of this work has been supported by the Stichting voor Fundamenteel Onderzoek der Materie (FOM) with financial support of the Nederlandse Organisatie voor Zuiver Wetenschappelijk Onderzoek (ZWO).

¹G. L. Pollack, *Rev. Mod. Phys.* **41**, 48 (1969).

²L. J. Challis, *J. Phys. C* **7**, 481 (1974).

³J. Weber, W. Sandmann, W. Dietsche, and H. Kinder, *Phys. Rev. Lett.* **40**, 1469 (1978).

⁴R. J. von Gutfeld and A. Nethercot, Jr., *Phys. Rev. Lett.* **12**, 641 (1964).

⁵H. J. Maris, B. Taylor, and C. Elbaum, *Phys. Rev. B* **3**, 1462 (1971).

⁶C. J. Guo and H. J. Maris, *Phys. Rev. Lett.* **29**, 855 (1972).

⁷R. A. Sherlock, A. F. G. Wyatt, N. G. Mills, and N. A. Lockerbie, *Phys. Rev. Lett.* **29**, 1299 (1972).

⁸T. J. B. Swanenburg and J. Wolter, *Phys. Rev. Lett.* **31**, 693 (1973).

⁹K. Andres, R. C. Dynes, and V. Narayanamurti, *Phys. Rev. Lett.* **31**, 687 (1973).

¹⁰O. Wels, *Z. Angew. Phys.* **26**, 325 (1969).

¹¹J. Maynard, *Phys. Rev. B* **14**, 3868 (1976).

¹²F. Rösch and O. Wels, *Z. Phys.* **B29**, 71 (1978).

¹³R. C. Dynes and V. Narayanamurti, *Phys. Rev. B* **12**, 1720 (1975).

¹⁴A. F. G. Wyatt, N. A. Lockerbie, and R. A. Sherlock, *Phys. Rev. Lett.* **33**, 1425 (1974).

¹⁵R. A. Sherlock, A. F. G. Wyatt, and N. A. Lockerbie, *J. Phys. C* **10**, 2567 (1977).

IV.3.3. TRANSMISSION OF BALLISTIC PHONON PULSES THROUGH A SOLID-LIQUID HE-II INTERFAC.

ABSTRACT

Results are presented on the transmission of ballistic longitudinal (L) and transverse (T) phonon pulses from sapphire into liquid He-II at a temperature $T \leq 0.25$ K. Fast response-time thin film transducers are used and broad-band (Planck-type) phonon radiation is employed. The conversion of L and T mode pulses at the interface into He-II is resolved using time-of-flight detection, with a detector located at some distance from the surface in bulk He-II. The ballistic part of the transmitted energy flux is measured as a function of generator power and hydrostatic He-II pressure. The transmission probability for T mode phonons is found to be higher than for the L mode. The data also indicate a strong frequency-down conversion at the interface, larger for the L mode than for the T mode.

I. Introduction

The problem of the Kapitza resistance¹⁻⁴ (heat transfer from a solid to liquid He-II) has received a rapidly increasing interest in recent years, both theoretically and experimentally. With the possibility of using phonon-pulse techniques⁵, it became possible to measure new, more microscopic parameters. Numerous phonon experiments at solid liquid He-II interfaces have been performed with this technique. However, most of the experiments performed used a phonon reflection technique, where an energy loss attributed to transmission into He-II is calculated and not measured directly⁶; therefore, a direct measurement of the energy transmitted into He-II is very much desirable. These phonon pulse experiments rely on ballistic phonon propagation in the media, where a phonon pulse can travel macroscopic

distances (1-10 mm) with negligible interaction with thermal excitations. For this reason, a phonon pulse transmission experiment through a solid-liquid He-II interface is intimately related to the phonon propagation characteristics of liquid He-II itself^{7,8}. In addition, ballistic phonon transmission experiments in He-II have recently attracted much interest in proving the existence of anomalous dispersion in the superfluid^{9,10}.

In the experiments involving transmission of phonon pulses in solid-liquid interfaces performed up to now, either the energy transported from the surface into the liquid was in a collective mode at $T = 1.3$ K (second sound)¹¹, or the time resolution was insufficient to resolve separately the ballistic transmission of the longitudinal (L) and transverse (T) polarised phonons from the solid¹². It is especially interesting to study how these modes are converted into the (longitudinal) phonon pulses in He-II. In this paper, we report on experiments of the transmission of ballistic phonon pulses from sapphire single crystals into bulk He-II at $T = 0.25$ K, where the conversion at the interface is time-resolved. Preliminary reports of these investigations have been published elsewhere¹³.

II. Phonon transmission in solid-He-II interfaces

The transmission of phonon energy through a solid-liquid interface (heat exchange) at low temperatures, is of considerable interest, from an experimental and theoretical as well as from the technological point of view. The still unsolved problem is why the so-called Kapitza thermal boundary resistance is 1 to 2 orders of magnitude smaller than theoretically calculated with the acoustic mismatch model (AMM)¹⁴ for phonon energies $\hbar\omega = kT$, with $0.1 < T < 10$ K. In the past years various modifications to the original AMM have been invoked to try to explain the enhanced transmission, including: Raleigh wave scattering,⁴ high-density liquid layers near the interface³, acoustic matching layers¹⁵, tunneling states of near surface He-atoms¹⁶ and He-atom desorption¹⁷. However, no clear picture emerges, perhaps with exception of the recent results of Weber Sandmann, Dietsche and Kinder¹⁸.

Most of the data on Kapitza resistances in solid-liquid He-II interfaces is acquired using conventional dc-thermal conductivity techniques. The first successful experiments in generating high-frequency superthermal phonons and detecting time-resolved longitudinal (L) and transverse (T) phonons according to their group velocity, were performed by von Gutfeld and Nethercot in pure dielectrics (sapphire, quartz)^{5,19,20}. Soon thereafter, a number of experiments was devised to apply this 'heat-pulse' technique to the Kapitza resistance problem^{6,11,21-27}.

The advantages of the pulse technique are obvious: i) separation of the L and T phonon propagation characteristics via time-of-flight detection, ii) the ability of injecting high power density pulses (with high phonon frequencies of 100 - 300 GHz) during short times (50 - 150 nsec) in materials with low thermal scattering, iii) geometric resolution by using small (1 mm²) transducers and thereby enabling the identification of heat flux from different directions (sidewall reflections, phonon focusing).

The majority of phonon pulse experiments for Kapitza resistance investigation are done in a pulse-reflection set-up⁶. Both generator and detector are located near each other on a crystal face and phonon pulses are reflected off the opposite surface, which is either kept in vacuum for reference purposes or covered with liquid helium to measure the signal loss, relative to the situation with vacuum. In this way a reflection coefficient R is found and the transmission probability T is given as $T = 1 - R$. The advantages of this reflection technique are: i) an environmental temperature of $T = 1.5$ K is sufficient, since thermal scattering in most dielectric crystals is then negligible, ii) the energy loss to thin condensed helium films can be measured and iii) other materials than helium can be studied for comparison. Some of the difficulties encountered are: i) in most cases the reflection is quite high, so the small difference between two rather large signals gives the relevant information, ii) the phonon focusing effects in solids²⁸ can have a significant influence on the detected signals, partly due to oblique propagation paths in the solid and iii) mode conversion (from T to L and vice versa) occurs at the interface as well as bulk scattering inside the crystal, thereby

sometimes making it difficult to extract valuable data for L modes, due to the necessary signal extrapolations. However, the main problem with the reflection experiments is the fact that no definite assignments can be made to the energy flux that has crossed the interface and is transferred into liquid helium. The problems with the interpretation of the phonon reflection are removed in an experiment measuring directly the transmitted phonon energy in He-II.

In this paper, we now concentrate on such a transmission experiment into He-II. As ballistic phonon propagation with mode resolution in both materials forming the interface is wanted, the phonon transport properties in liquid He-II are highly important^{10,29-31}.

The phonon properties of liquid Helium and related experiments are now discussed briefly. Due to the intense phonon-roton interaction (and the resulting small phonon mean free path) in He-II at $T = 1.5$ K, a direct phonon pulse transmission experiment is not straightforward at temperatures above $T = 1$ K, since the energy transport in He-II then appears as a collective mode (second sound). In one experiment these second sound pulses, generated at the solid-liquid interface by ballistic phonons, have been used for a study of the Kapitza resistance¹¹. This collective mode is thermally frozen out at much lower temperatures, $T < 0.35$ K, leaving only phonons as thermal excitations in He-II and making ballistic transport in He-II equally possible as in pure solids^{7,8}. An experiment which uses this ballistic propagation in He-II is the phonon transmission experiment of Sherlock, Wyatt, Mills and Lockerbie from NaF to He-II at $T = 0.1$ K. However, no mode resolution was obtained because of the use of slow carbon detectors, having some $\mu\text{sec.}$ response-time. In the work reported here, fast (10 - 25 nsec. response-time) metallic film detectors are used¹⁹. Also the generator pulses are a factor of 10 - 100 shorter in our case, providing sufficient time resolution to detect transmission of L and T modes separately.

The three main experimental parameters which can be varied in this type of low temperature phonon experiment are 1) generator power density, 11) He-II pressure and 111) environmental He-II temperature.

The generator power density determines the phonon radiation frequency distribution in the solid (its 'effective' heater temperature

T_h) generally calculated using modified acoustic mismatch models^{32,33}. For the power levels used here ($< 3.5 \text{ W/mm}^2$) this frequency spectrum is experimentally verified to be of black-body nature (Planck radiation)³⁴. The effective heater temperature can therefore be interpreted as a parameter specifying a black-body radiation spectrum according to the Stephan-Boltzmann formula. In this broad-band thermal radiation model the power density goes with T_h^4 and the dominant phonon frequency (ω_m) is given by $\hbar\omega_m = 2.8 kT_h$; the radiation bandwidth is about equal to the dominant frequency ω_m . The phonon pulses generated by the heater travel down the crystal with low thermal scattering, retaining their spectral distribution but 'diluting' in intensity.

A change in pressure on the superfluid He-II influences only slightly the dispersion curve of He-II, but modifies dramatically the possible phonon scattering processes^{31,36,37}. It is now well-established^{9,10} that at high pressures $p > 20$ bar the dispersion is normal (downward) for all energies, or $v_g(E) < c_0$. ($v_g(E)$ being the energy dependent group velocity $d\omega/dk$ and c_0 the long wavelength sound velocity.) At lower pressures, $p < 10$ bar, anomalous (upward) dispersion exists, with an energy region on the $\omega(k)$ curve where $v_g(E) > c_0$; this leads to the existence of a unique three phonon decay process (3PP) and a resulting small phonon mean free path (mfp) for phonons of corresponding energies³¹. The environmental He-II temperature describes the population in the phonon and roton systems and thus controls the phonon roton interaction which becomes rapidly important for $T > 0.35$ K. For lower T , thermal He-II is essentially described by a phonon system, as is already mentioned before.

III. Experimental details

The experimental arrangement used for ballistic phonon transmission experiments is shown in Fig. 1. Evaporated thin metallic films are employed as generator and detector for the phonon pulses⁵. The generator consists of a $1 \times 1 \text{ mm}^2$ constantan film of nominal 50 ohm resistance (thickness 150 \AA), connected to its coaxial line with evaporated (3500 \AA thick) Sn electrodes. In some cases, this heater

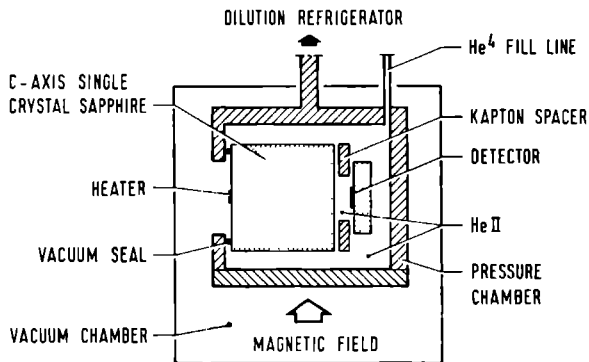


FIG. 1. Experimental arrangement for detection of ballistic phonon transmission from sapphire into liquid He-II.

film was covered by a 550 \AA layer of silicon for protection against degradation. The detector is a thin superconductive aluminum film of similar dimensions and a thickness of $150 - 250 \text{ \AA}$, evaporated onto a sapphire substrate. The detector is operated at the resistive transition at low temperatures ($T/T_c = 0.1$, for $T_c(\text{Al}) \cong 1.3 - 1.5 \text{ K}$) by applying a magnetic field (1.0 T) parallel to the film. A small dc current is passed through the film to measure its resistance variation, and incident phonon pulses are then detected as voltage pulses over the film due to the high temperature sensitivity of the resistance at the superconductive transition.

Sapphire single crystals were chosen for the transmission measurements, since this material has frequently been used in phonon pulse experiments^{5,6,38,39}, thus providing data for comparison and its acoustic properties are very well described⁴⁰.

The crystals were one Verneuil (V) and two Czochralski (CZ) grown cylindrical single crystals with a length of 20, 15, 8 mm and a diameter of 10, 15, 15 mm respectively. The best resolved phonon

pulses were obtained with the 15 mm diameter crystals; this has been measured by evaporating a detector on the crystal face opposite the generator. The cylindrical crystal axis was within 1° parallel to the crystallographic c-axis; the transverse phonon mode is therefore degenerated in velocity^{20,40}. From conventional thermal conductivity measurements the phonon mean free path (mfp) in the V crystal was found to be 10 mm (boundary scattering regime). From phonon pulse data, the two CZ crystals are believed to have an even longer mfp.

For the transmission measurements with the CZ crystals, the heater film on the sapphire was kept with the 'back'-side of the film in a high-vacuum environment of the dilution refrigerator isolation to ensure that all phonon energy is directed into the crystal. For this purpose, the 15 mm crystal face was bolted against a stainless steel flange using an indium seal construction.

The time-of-flight patterns for ballistic phonon propagation in the crystals were measured several times using different sets of generator and detector films. No inconsistency was found for Al, Sn or In detectors of thickness from 150 to 550 Å and for environmental temperatures of 0.1 or 1.5 K. The arrival of such a pulse signal is shown in the lower trace of Fig. 3. For measurements on the transfer of phonon pulses from these crystals into liquid He-II, the sapphire substrates with the detector films were mounted in an open teflon holder, separated from the transmitting crystal face by a kapton spacer at a distance of about 0.5 mm and accurately aligned parallel to the generator film. The holder is designed to be free of sidewall reflections which might interfere with the direct phonon beam during the first 20 μsec. The spacer distance was accurately determined at $T = 1.5$ K by measurements of the round trip time of second sound pulse echo's in the He-II space, generated by phonon pulses incident on the interface⁴¹ (Fig. 2). The second sound velocity does not vary much around $T = 1.5$ K, and its value is taken from data on CW second sound⁴². The accuracy of this length calibration is 15 μm at the actual spacer distance of 500 μm. This assembly is mounted on the detachable flange of a stainless steel pressure chamber of 25 cm³ internal volume and sealed with an indium-O-ring construction. The

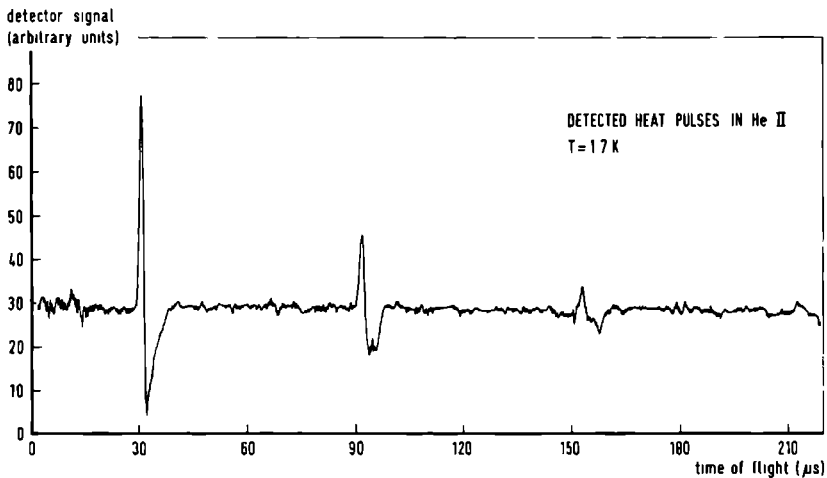


FIG. 2. Detected second sound pulses, generated at the sapphire-He-II interface by incident ballistic phonon pulses, using the experimental arrangement of Fig. 1.

experimental chamber is attached to the mixing chamber of a home-made, simple He^3 - He^4 dilution refrigerator and cooled down to $T = 0.1$ K. Heat exchange between the mixing chamber and the experimental cell is done with an 18 mm diameter copper rod with direct access in both chambers; each end of rod has some 50 cm^2 of copper fins as heat exchange area. The refrigerator has a single 1 m long concentric tube heat exchanger. With the experimental cell attached, the cooling power is about $10 \mu\text{W}$ at $T = 0.1$ K. The He-II cell temperature is monitored and stabilized by means of a Speer carbon resistor, immersed in liquid He-II, which was previously calibrated against a CMN thermometer using an AC susceptibility bridge. The error in temperature induced by magnetoresistance can amount to a maximum of 15 mK. After passing over liquid nitrogen cooled zeolite traps, high-purity 5N5 helium gas is condensed via a capillary into the cell. Hydrostatic pressure up to the solidification point (25.5 bar at $T = 0.1$ K) can be applied through a closed-loop gas handling system. Electrical contacts

to the films are made using miniature coaxial cables with a bandwidth of 35 MHz. Current pulses of width of 50 - 150 nsec and an amplitude of 0.5 - 15 V are used to excite the heater film with a Hewlett-Packard 8015A pulse generator.

After ballistic propagation and mode separation in the crystal, the longitudinal (L) and transverse (T) phonon pulses are both converted to longitudinal phonons in liquid He-II, and these converted pulses are sensed by the detector film, again after ballistic propagation through He-II. The pulse signals are wide-band amplified and digitized by a Biomation 8100 transient recorder (with a time resolution of 10 nsec) and subsequently averaged in a digital signal averager. To avoid excessive heating in the experimental cell, most of the time a pulse repetition rate of 1 - 10 Hz was used; if a higher rate could be tolerated, a PAR 160 boxcar integrator was used. If needed, the electromagnetic crosstalk from the generator pulse was suppressed by averaging successive trains of carefully adjusted pulses with equal amplitude but of opposite polarity. After averaging 1000 sweeps, this system is capable of detecting signals of the order of microvolts and 150 nsec duration, generated with a power density of 1 W/mm^2 ($0.05 \text{ } \mu\text{J/pulse}$) after propagation through the 15 mm crystal, the solid-liquid interface and 0.5 mm of liquid He-II, with a signal to noise ratio of 10. However, sometimes 16,000 sweeps were necessary to recover adequately the signals with a very low intensity. The crystal surfaces were carefully cleaned, as it is customary for the evaporation of metallic films on sapphire material; but no special precautions were taken. The surfaces were mechanically polished by the manufacturer. Removing used or damaged films was done in acids, neutralizing in a decontaminant (decon), flushing and cleaning with spraying pure ethanol, followed by a glow-discharge. The claimed surface roughness is better than $1 \text{ } \mu\text{m}$, with a dislocation density of less than $10^3/\text{cm}^2$.

IV. Experimental results and analysis

For reference purposes, the time-of-flight signals for the three c-axis crystals were measured several times, before and after the helium transmission experiments and with different sets of equally dimensioned transducer films, evaporated on opposite faces of the crystal. These measurements provide the flight-times for the phonon modes, the L/T mode density ratio in the crystal and some indication of the energy flux incident on the crystal face. The shorter crystals (15 and 8 mm long) provided better mode separation from sidewall echo's. For these shorter crystals, the He-transmission experiments were performed with the heater film being vacuum-isolated. Therefore, most of the following analysis refers to measurements on these crystals. The observed intensity ratio of L and T mode phonons (hereafter referred to as 'L/T-ratio') was always found to be 0.31 ± 0.02 for a pulse width of 50 - 300 nsec and pulse power densities up to 2.0 W/mm^2 . Theoretical calculations of Rösch and Weis for propagation along the c-axis of sapphire, using comparable film dimensions, give a value of 0.33 for this ratio⁴⁰. In the lower trace of Fig. 3 the time-of-flight signal for a 15 mm sapphire is shown.

Ballistic phonon transport in superfluid He-II is possible for temperatures $T < 0.35 \text{ K}$. As explained in section II, at these temperatures the roton energy levels are depopulated. The reason why this occurs at such low temperatures, compared with the minimum roton excitation energy of 8 K, is the very high density of states $D_r(E)$ for the rotons with a low group velocity $v_g(E) = dE/dk$:
 $D_r(E) \propto v_g^{-1}(E) = dk/dE$ ^{43,44}. For $T < 0.35 \text{ K}$, the liquid behaves as a pure, isotropic dielectric with one longitudinal acoustic phonon mode, showing anomalous dispersion at low pressures as discussed in section II. Excellent ballistic phonon signals were detected in experiments with thin film transducers mounted opposite each other at a distance of 2.44 mm in a liquid He-II cell.

For the study of the transmission of phonon pulses from sapphire into He-II at $T < 0.35$ the experimental set-up shown in Fig. 1 is used. Following the generator pulse, the phonon flux propagates to the interface where both L and T mode phonons are converted to L mode

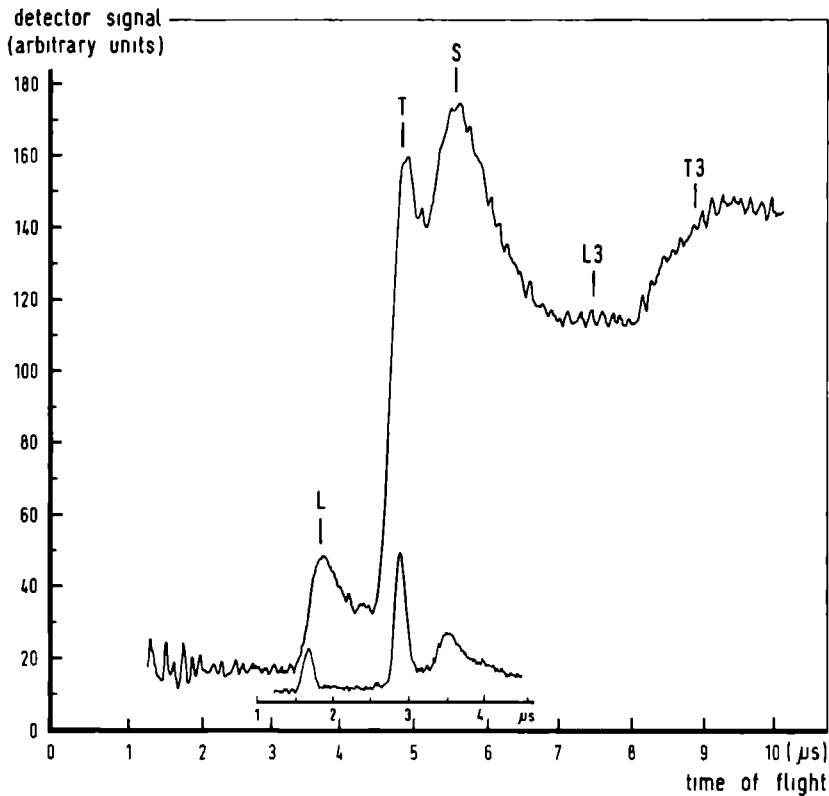


FIG. 3. Ballistic time-of-flight signal detected with the experimental arrangement of Fig. 1. Upper trace: longitudinal phonon pulses in He-II, excited by longitudinal (L), transverse (T) and sidewall reflected (S) phonon pulses in sapphire (He-II temperature: $T = 0.22$ K, He-II pressure: $p = 21$ bar, generator pulse width: 150 nsec, pulse power density: 1.48 W/mm²). Lower trace: L,T,S phonon time-of-flight signal with the detector on the sapphire face, shifted in time according to the propagation delay in liquid He-II.

phonons in liquid He-II, and these two pulses are detected after additional ballistic flight in He-II. A typical time-of-flight signal for converted L and T phonons is shown in Fig. 3. The time positions indicated are calculated transit times, using flight-times in the crystal, known phonon velocity in liquid He-II²⁹ and the detector-crystal separation as measured at T = 1.5 K using second sound. The pressure dependent phonon velocity in He-II gives an additional check on the detector distance from the surface (Fig. 4). The measured times

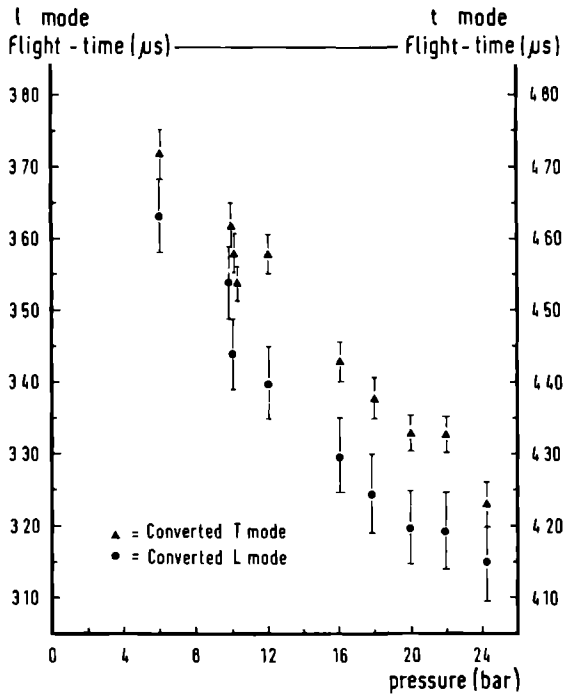


FIG. 4. Pressure dependence of the arrival time of converted ballistic L and T modes (He-II temperature: T = 0.23 K, pulse power density: 0.7 W/mm²).

coincide within 50 nsec with the expected arrival times for ballistic propagation in sapphire and in He-II. Therefore it can be concluded that the conversion mechanism does not delay the energy transfer for more than this time interval. Since the sidewall-reflected (S) pulse is incident at the interface at oblique angles and is strongly subject to phonon focusing²⁸ we concentrate on the direct transmitted L and T modes. In contrast with earlier experiments¹², where carbon detectors were used, the high time-resolution thin films and the short generator pulses (50 - 150 nsec) used here, enable us to resolve in the liquid the excitations originating from L and T phonons in the solid separately. The detected signals labeled L and T were found to scale linearly with bias current in the range used (10 - 100 μ A), indicating that there is no sharp detection threshold and that dc-heating by the bias current through the detector ($< 1 \mu$ W) is not important. A comparison of pulse area's is hindered by necessary extrapolations of the signals and therefore we limit ourselves to the peak intensities of the signals; in cases where the extrapolation was free of error, a linear relation between peak intensity and signal area was found. The converted L and T signals depend linearly on generator pulse width (i.e. pulse-energy) in the range of 50 - 500 nsec, see Fig. 5. For all measurements reported here, a pulse width of 150 nsec was used.

The intensities of converted L and T phonon pulses and their intensity ratio (L/T ratio) are plotted as a function of generator power density in Fig. 6 for an environmental He-II temperature of $T = 0.23$ K and a He-II pressure of 24 bar, just below the solidification point. The indicated effective heater temperature is calculated from the pulse power density under acoustic mismatch conditions³², using phonon emissivities of 0.17 - 0.20 for the constantan-sapphire interface. We find a linear dependence up to 3.2 W/mm^2 . However, there appears a break in slope for the signal originating from the T mode in the solid at a calculated heater temperature of 8.3 K. Within experimental accuracy, no such break could be found in the L mode curve at the same power density. This break in slope is not due to detector saturation as the signal is linear below and above 0.8 W/mm^2 , and the signal intensity depends linearly on pulse energy (Fig. 5) up to signal levels above the maximum level shown in Fig. 6. The estimated temperature of

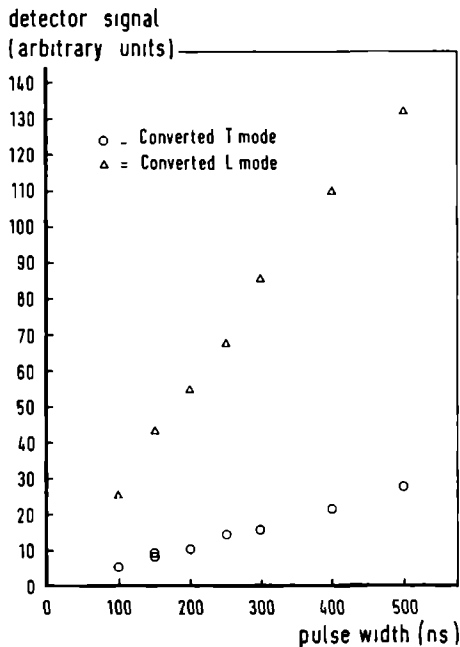


FIG. 5. Intensity of converted L and T modes as a function of generator pulse width (He-II temperature: $T = 0.23$ K, He-II pressure: $p = 24.2$ bar, pulse power density: 1.2 W/mm²).

the heater at the breakpoint is about 0.5 K higher than minimum energy for roton excitation at the He-II temperature and pressure used. This might indicate that a part of the transverse energy flux at the surface couples directly to roton excitations in liquid He-II. This possible direct roton excitation is not further investigated here.

As can be seen in Fig. 6b, the L/T ratio amounts to 0.20 ± 0.02 and 0.24 ± 0.02 respectively for power densities below and above 0.8 W/mm², which is to be compared with a constant value of 0.31 ± 0.02 found in the crystal itself. Since there are no frequency selective phonon decay processes possible in He-II in the regime of normal dis-

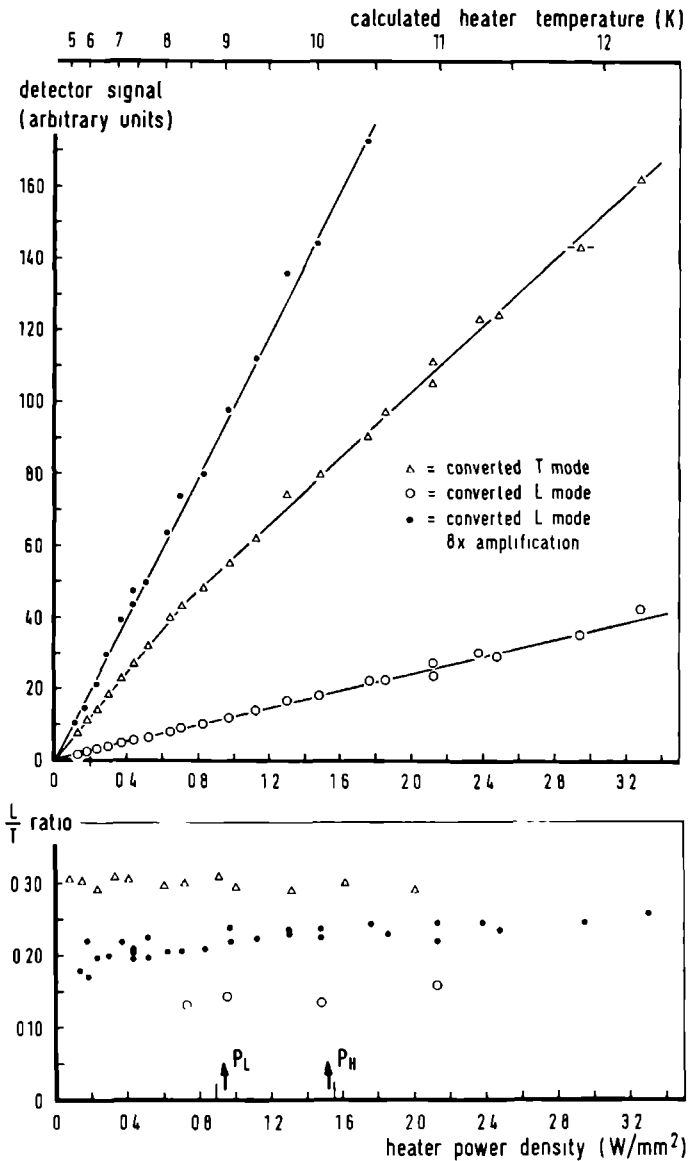
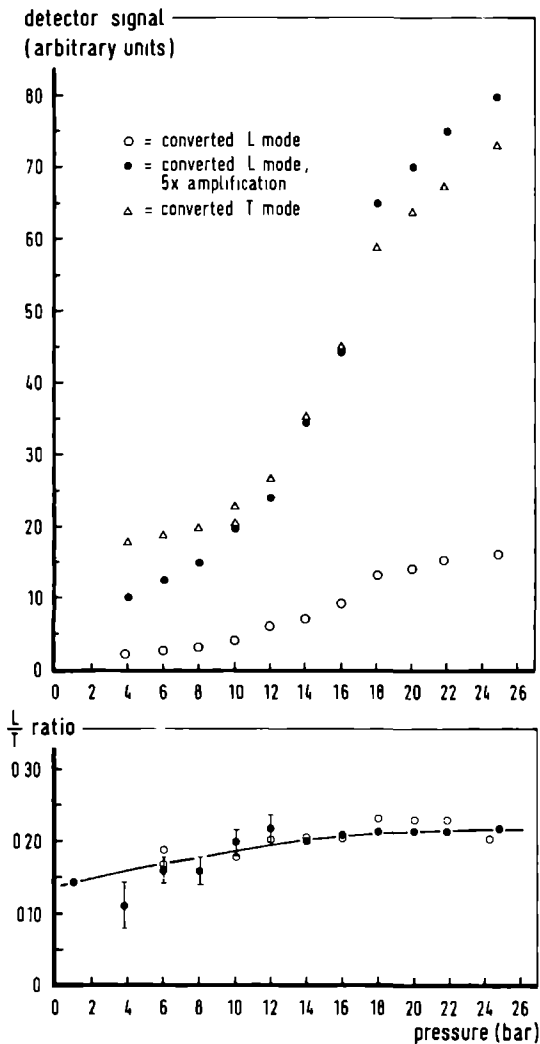


FIG. 6a. Intensity of converted L and T modes as a function of heater power density (He-II temperature: $T = 0.23$ K, He-II pressure: $p = 24$ bar, pulse width: 150 nsec).

FIG. 6b. Intensity ratio of converted L and T modes as a function of generator power density. Triangles with detector film onto sapphire crystal, closed symbols: ratio of signals shown in Fig. 6a (He-II pressure: 24 bar); open symbols: typical data for the ratio at a He-II pressure of 1 bar. P_L and P_H refer to the power levels used in Fig. 7.

persion (high pressure of 24 bar), we attribute this decrease from 0.31 to 0.22 in the L/T ratio to the phonon coupling process at the interface. From this it follows, that the ballistic transmission for T mode phonons into He-II is a factor of 1.5 (at high power densities) to 1.2 (at low power densities) more effective than for L mode phonons. This is in qualitative agreement with the results from pulse reflection experiments on similar surfaces by Maris and Folinsee^{6,26}, but in contrast with second sound excitation experiments of Swanenburg and Wolter¹¹ who found equal transmission coefficients for both modes from a silicon surface into He-II at $T = 1.3$ K. On basis of the acoustic mismatch theory² the strong conversion of the T mode is not expected. In addition, recent experiments by Weber, Sandmann, Dietsche and Kinder¹⁸ have shown that reflection coefficients from a cleaved LiF surface are found, which are in close agreement with theoretically predicted values.

At a He-II pressure of 1 bar we find the converted L/T ratio to be decreased to 0.15 ± 0.01 , as indicated by the data points in Fig. 6. In this situation, the signal is too weak to discern any structure around 0.8 W/mm^2 . This effect of pressure on the pulse transmission is more clearly displayed in Fig. 7, where the converted L and T mode signals and their ratio are plotted as a function of He-II pressure for two generator power densities of 1.50 and 0.92 W/mm^2 . In both series, a decrease of a factor of 4.5 ± 0.2 in signal amplitude on lowering the pressure below 10 bar is found. This reflects the onset of anomalous dispersion at low He-II pressures^{9,10,36,37}; the anomalous dispersion allows a spontaneous three phonon decay process (3PP) to occur and hence drastically shortens the phonon mean free path for low energy phonons. Since this 3PP applies equally to both converted L and T mode phonons (being both longitudinal phonons in He-II), no change in converted L/T ratio is expected if the frequency distributions in both these pulses are described by the same black-body temperature T_h . Following this line of arguments, the decrease in detected L/T ratio gives an indication for the existence of different frequency distributions (unequal 'pulse-temperatures') in the two pulses. As the spectral influence of He-II is identical on both modes,



this effect has to originate from conversion at the interface. In this way, direct evidence for inelastic energy transfer at the solid-liquid interface can be found. For the two power densities used, the decrease in L/T ratio is the same within the experimental error of 0.02: from 0.22 at 24 bar to 0.15 at 1 bar. Due to the fourth root dependence of heater temperature on power density, no large difference is expected.

The experiments by Maris²² on pressurized He-II at $T = 1.5$ K did not reveal any pressure effect on the reflection of both L and T modes. However, no change in the signal at $p = 14$ bar is expected in their results as this is related to inherent properties in phonon transport in bulk He-II. A pressure dependent transfer mechanism, different for L and T modes, is not likely to account for these results (sharp decrease at 14 bar and shift in L/T ratio from 0.22 to 0.15) because a monotonic pressure influence is then expected due to the gradual change in He-II density with pressure⁵². Evidence for frequency down-conversion of phonons at the interface can be derived from the fact that at lower pressures ($p < 10$ bar) liquid He-II is known to have a frequency selective mean free path for phonon excitations (spontaneous 3PP). In this context it is significant to note that the L/T ratio begins to decrease for $p < 10$ bar. From the experimental results of other groups indicating that the 3PP-cut-off energy is linearly dependent on pressure^{9,10,36}, approaching zero energy at $p = 18$ bar and its full value at $p = 0$ bar, we find that the lower frequencies in the transmitted distributions will be first attacked by the 3PP on lowering the pressure below $p = 18$ bar. From the measured pressure dependent shift in the L/T ratio one concludes that the L mode is more effectively down converted in frequency than the T mode. In pulse reflection experiments with narrow-band phonon radiation, Dietsche and Kinder found evidence for down-conversion at solid-liquid interfaces; however, their measurements were limited to T mode reflection only^{25,28}.

Using certain assumptions, it is possible to get quantitative estimates on the relevant frequency distributions from these experiments. The broad-band pulse technique employed here has a radiation bandwidth of $\Delta E = 2.8 kT_h$ ³², which is about equal to the dominant

energy in the Planck radiation spectrum. A detailed and sophisticated interpretation of our data should invoke a deconvolution of the time-of-flight data from the generator spectrum^{45,46}. Such an analysis requires three main functions: i) the incident phonon spectrum on the interface, which can be assumed to be a Planck type distribution, ii) a model for the energy absorption at the detector film and iii) a very accurate description of the highly dispersive phonon group velocity $v_g(E)$ and the relevant cut-off energy E_c in He-II at pressures between 1 and 24 bar. Nevertheless, a rather crude estimate can be made for the frequency shift in the spectrum by assuming that it can be simply described with a change in the pulse-temperature of the black-body radiation. We make use of the fact that at $p = 24$ bar the phonon mean free path in He-II is long ($mfp > 1$ mm) for all energies (normal dispersion). From the decrease in the L/T ratio from 0.22 to 0.15, we estimate that the converted L mode pulse is 1.2 ± 0.2 K lower in temperature than the converted T mode. Thereby it is assumed that the L/T ratio at 24 bar is true and that it leads to the same temperature for both pulse signals. This temperature difference is found by adjusting the slopes of the power plot at $p = 1$ bar until a ratio of 0.22 is obtained. The difference in pulse-temperature T_h , and also the tentative explanation for the break in slope in Fig. 6, obviously rely very much on the validity of the calculated heater temperatures, leading to a description of the phonon spectra entering the liquid.

There exists some evidence to prove that the acoustic mismatch model is appropriate to describe the heat transport through solid-solid interfaces at the power levels used here^{33,34}. However, this model seems to fail to explain phonon transmission experiments through solid-liquid interfaces⁴⁵. As becomes clear from the following reasoning, this would imply that the heater-temperatures indicated in Fig. 6, are not adequate to describe the phonon spectra detected in He-II. From Fig. 6 it can be noted that the signal intensity increases linearly with power (bolometric response), as expected and verified for this type of detectors⁴⁷. If we, however, rely on the temperature-scale of Fig. 6 to describe the frequency distribution entering the liquid and we assume elastic energy transfer, a linear power depen-

dence is not expected for the ballistic phonon pulse. Due to the bandwidth of the thermal radiation, at $T_h = 10.2$ K a large fraction of the energy in the pulse is associated with energies larger than 12.5 K. This fraction cannot couple directly to phonon excitation in He-II. Therefore, a strong, decreasing non-linear power dependence should result for calculated heater temperatures $T_h > 5$ K, since the phonon intensity at frequencies above the dominant frequency $\omega_m = 2.8 kT_h/\hbar$ increases very rapidly with T_h ³². Therefore, the linear power dependence observed in our experiments suggests that the pulse temperature of the phonon flux in the liquid is substantially lower than T_h of the pulse incident from the solid side, calculated from the generator power density.

Most of the experiments using thin films give no reason to doubt the validity of the AMM at the power levels used here^{33,34}. The AMM gives a value of 0.18 for the phonon emissivity from the constantan heater to the sapphire crystal. The assumption of a perfect match of the heater to the crystal would therefore bring down the indicated temperatures in Fig. 6 with a factor of 1.5 over the whole range⁴⁷. Such a matching, although questionable, would provide a better fit to our data than the AMM prediction. By retaining the AMM and thus the T_h in the solid as calculated in Fig. 6, we have to consider the energy transfer process at the interface as the source of the energy-down conversion. In a phonon emission experiment through He-II at 24 bar with a thin film heater and a carbon resistor as detector, a considerable difference was found in T_h , if T_h was calculated from the AMM, or from the pulse-temperature, deconvolved from the time-of-flight signals⁴⁵. In this analysis the dispersive phonon group velocity $v_g(E)$ was explicitly taken into account. If we extrapolate these results from 0.25 W/mm^2 to 0.8 W/mm^2 , our calculated T_h in the liquid scales down a factor of 3.5 at this power density and becomes 2.4 K. This explains the linear power dependence illustrated in Fig. 6, since for this pulse-temperature, taking the radiation bandwidth $\Delta E = 2.8 kT_h$ into account, all frequencies in the Planck-like distribution can couple into He-II phonons. For this same reason, the break in slope appears approximately at the minimum roton energy.

However, no sharp break in slope is expected, even with the high density of roton states available at 8 K.

In addition to the relative intensity of the converted L and T modes, the absolute magnitude of the transmission coefficient is of considerable interest. By measuring the loss of signal in pulse reflection experiments, one usually finds transmission coefficients in the range from 0.1 to 0.6²³, in contrast to the AMM. For the T mode transmission, one finds always high values²⁶. However, Weber, Sandmann, Dietsche and Kinder have performed very interesting reflectivity experiments on surfaces, freshly cleaved in vacuum at low temperatures¹⁸; they found phonon transmission coefficients smaller than 0.05, which is in close agreement with the predictions from the AMM. Therefore, the enhanced phonon transmission found in most experiments performed on 'dirty' (not-vacuum cleaved) surfaces could be attributed to non-intrinsic properties of the surface (i.e. physical imperfections, adsorbed gases, etc.). However, from the reflection experiments one cannot conclude unambiguously if the measured energy loss is due to excitations (phonons) in the bulk liquid or if the energy disappears in some other way. Only transmission experiments measure directly the energy propagating away from the surface, but these experiments have the difficulty that the detected signal intensities have to be related to the actual flux incident on the interface in a clear-cut, well-defined way. The main problem in making quantitative statements is the unknown detection efficiency of the He-II phonons in the detector film. In time-of-flight signals as illustrated in Fig. 3, one can usually discern two pulse-echo's in the liquid He-sample, situated between crystal and detector; this indicates a rather high reflection from the liquid to the solid. If we compare signal intensities received with detectors on the crystal-face or with a detector in liquid He-II, 0.5 mm away from the crystal face, and take the corresponding different coupling efficiencies into account, we find for the same generator power density ($< 3.5 \text{ W/mm}^2$) signal levels which are about two orders of magnitude lower in the liquid than in the solid. For an absolute determination of the transmission coefficient, the energy transfer efficiency from the liquid to the detector has to be known. Although the present status of our experi-

ment does not allow an absolute determination of the transmission coefficient, some rough estimates can be made on the bases of comparable detector situations. If we compare our ballistic phonon propagation experiments in superfluid He-II at $T = 0.1$ K with transmission experiments through sapphire single crystals, using comparable power levels, transducer geometries and sample lengths, we find the signal intensities in He-II not more than a factor of 10 lower than in the sapphire. Therefore, we can estimate that the transmission coefficient into He-II is in the range of 0.03 to 0.10. This is considerably lower than the values deduced from conventional reflection experiments^{22,23,26}, but higher than the values found on freshly cleaved surfaces¹⁸. In an experiment involving simultaneously two detectors, one on the crystal-face and the other at a distance of 0.7 mm in liquid He-II and both located at an angle of 5° off the crystal c-axis direction, the same large difference in signal intensities has been measured, however, no detailed data on power density were taken in this run.

Within the constraints mentioned above, our direct transmission experiments lead to a lower transmission efficiency than deduced from most of the conventional pulse reflection experiments, at least as far as the ballistic phonons in He-II are concerned. Our findings are therefore in better agreement with the AMM, and not inconsistent with the reflection measurements on freshly cleaved surfaces¹⁸. Obviously, a direct measurement of the detector sensitivity to the energy from the liquid would be a great improvement.

V. Summary and conclusions

Using fast phonon pulse techniques, we have measured the transmission of L and T mode phonons separately from sapphire into liquid He-II at $T = 0.25$ K, under ballistic energy transport conditions in both media. The results indicate an enhanced transmission probability of the T mode compared with the L mode. From the measured influence of the He-II pressure we deduce evidence for frequency down-conversion at the interface, and assuming a black-body radiation spectrum in the phonon pulse an estimate is made of the change in frequency distribu-

tions. It should be interesting to persue this type of experiments by using monochromatic phonon radiation, simultaneous measurement of reflection and transmission and studying the influence of the surfaces (i.e. freshly cleaved, covered with evaporated thin matching layers or covered with absorbed gases under controlled conditions).

References

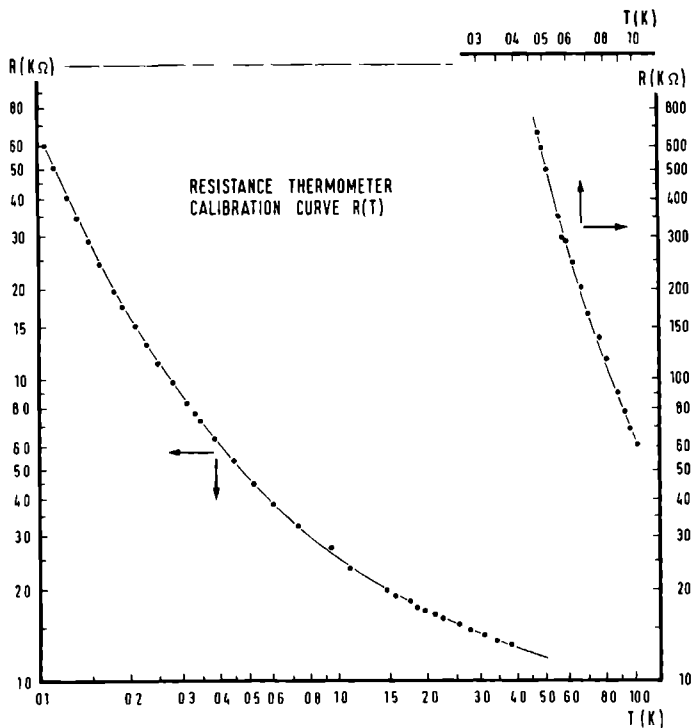
1. P.L. Kapitza, J. Phys. (USSR) 4, 181 (1941).
2. I.M. Khalatnikov, Zh. Eksp. Teor. Fiz. 22, 687 (1952), and Introduction to the theory of superfluid helium (Benjamin, New York, 1965), Ch. 23.
3. G.L. Pollack, Rev. Mod. Phys. 41, 48 (1969).
4. L.J. Challis, J. Phys. C 7, 481 (1974).
5. R.J. von Gutfeld and A.H. Nethercot Jr., Phys. Rev. Lett. 12, 641 (1964).
6. C.J. Guo and H.J. Maris, Phys. Rev. Lett. 29, 855 (1972).
7. R.W. Guernsey and K. Luszczynski, Phys. Rev. A 3, 1052 (1971).
8. V. Narayanamurti, R.C. Dynes and K. Andres, Phys. Rev. B 11, 2500 (1975).
9. N.G. Mills, R.A. Sherlock and A.F.G. Wyatt, Phys. Rev. Lett. 32, 978 (1974).
10. R.C. Dynes and V. Narayanamurti, Phys. Rev. B 12, 1720 (1975).
11. T.J.B. Swanenburg and J. Wolter, Phys. Rev. Lett. 31, 693 (1973).
12. R.A. Sherlock, A.F.G. Wyatt, N.G. Mills and N.A. Lockerbie, Phys. Rev. Lett. 29, 1299 (1972).
13. H.W.M. Salemink, H. van Kempen and P. Wyder, Phys. Rev. Lett. 41, 1733 (1978); J. Physique (Paris), C6-326, (1978); H.W.M. Salemink, Thesis, University of Nijmegen, The Netherlands, 1979.
14. W.A. Little, Can. J. Phys. 37, 334 (1959).
15. J.L. Opsal and G.L. Pollack, Phys. Rev. A 9, 2227 (1974).
16. T. Yakayama, J. Phys. C 10, 3273 (1977).
17. R.C. Johnson and W.A. Little, Phys. Rev. 130, 596 (1963).
18. J. Weber, W. Sandmann, W. Dietsche and H. Kinder, Phys. Rev. Lett. 40, 1469 (1978).
19. R.J. von Gutfeld, A.H. Nethercot and J.A. Armstrong, Phys. Rev. 142, 436 (1966).
20. R.J. von Gutfeld, Physical Acoustics, edited by W.P. Mason (Academic, New York, 1968), Vol. 5, p. 223.
21. T. Ishiguro and T.A. Fjeldly, Phys. Lett. 45A, 127 (1973).
22. J.S. Buechner and H.J. Maris, Phys. Rev. Lett. 34, 316 (1975).

23. C.J. Guo and H.J. Maris, Phys. Rev. A 10, 960 (1974).
24. A.R. Long, R.A. Sherlock and A.F.G. Wyatt, J. Low Temp. Phys. 15, 523 (1974).
25. W. Dietsche and H. Kinder, J. Low Temp. Phys. 23, 27 (1976).
26. J.T. Folinsbee and J.P. Harrison, J. Low Temp. Phys. 32, 469 (1978).
27. H.J. Trumpp, K. Lassman and W. Eisenmenger, Phys. Lett. 41A, 431 (1972).
28. H.J. Maris, B. Taylor and C. Elbaum, Phys. Rev. B 3, 1462 (1971).
29. R.C. Dynes, V. Narayanamurti and K. Andres, Phys. Rev. Lett. 30, 1129 (1973).
30. A.F.G. Wyatt, N.A. Lockerbie and R.A. Sherlock, Phys. Rev. Lett. 33, 1425 (1974).
31. H.J. Maris, Rev. Mod. Phys. 49, 341 (1977).
32. O. Weis, Z. Angew. Phys. 26, 325 (1969).
33. P. Herth and O. Weis, Z. Angew. Phys. 29, 101 (1970).
34. W.E. Bron and W. Grill, Phys. Rev. B 16, 5303 (1977).
35. A.D.B. Woods and R.A. Cowley, Rep. Prog. Phys. 36, 1135 (1973).
36. J. Jäckle and K.W. Kehr, Phys. Rev. Lett. 27, 654 (1971).
37. H.J. Maris and W.E. Massey, Phys. Rev. Lett. 25, 220 (1970).
38. H. Kinder and W. Dietsche, Phys. Rev. Lett. 33, 578 (1974).
39. A.H. Dayem and W. Eisenmenger, Phys. Rev. Lett. 18, 125 (1967).
40. F. Rösch and O. Weis, Z. Physik B 29, 71 (1978).
41. R.W. Guernsey, K. Luszczynski and W. Mitchell, Cryogenics 7, 110 (1967).
42. J. Maynard, Phys. Rev. B 14, 3868 (1976).
43. R.C. Dynes and V. Narayanamurti, Proceedings of the EPS Topical Conference on Liquid and Solid Helium, July 1974, Haifa (edited by C. Kuper, S. Lipson and M. Revzon), J. Wiley, New York and Israel University Press.
44. R.W. Guernsey Jr., Ph.D. Thesis, Washington University, St. Louis, 1968 (unpublished).
45. R.A. Sherlock, A.F.G. Wyatt and N.A. Lockerbie, J. Phys. C 10, 2567 (1977).
46. M.P.W. Strandberg and L.R. Fox, Phys. Lett. 62A, 151 (1977).

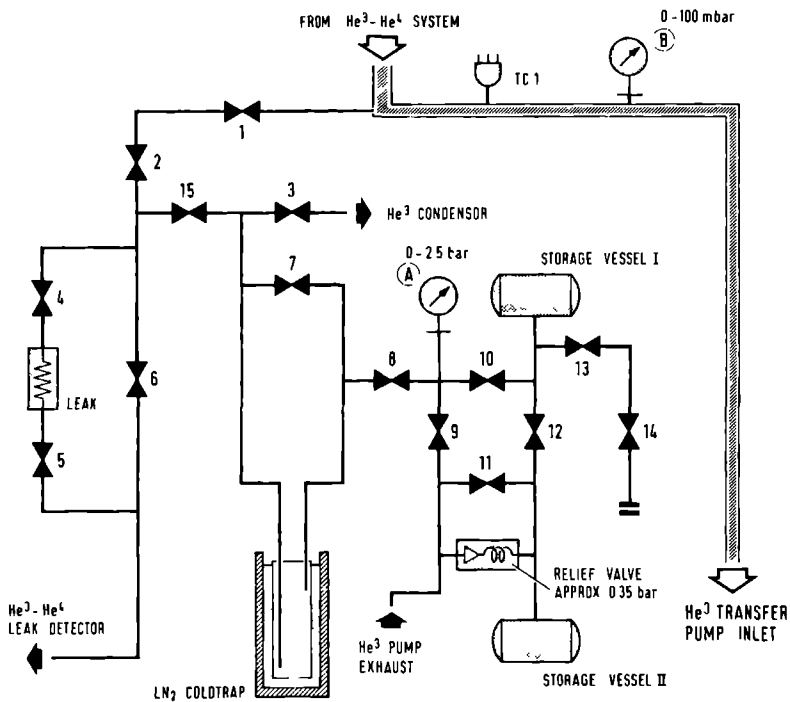
47. R.C. Dynes and V. Narayanamurti, Phys. Rev. B 6, 143 (1972).
48. N. Perrin and H. Budd, Phys. Rev. Lett. 28, 1701 (1972).

V. APPENDIX

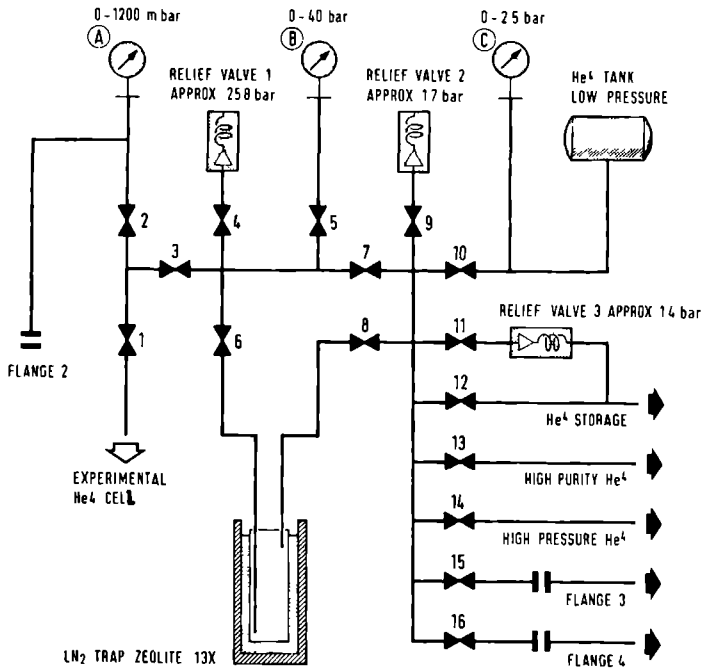
- V.1 Calibration curve of the thermometer in the dilution refrigerator.
- V.2 He³-He⁴ gas handling system of the dilution refrigerator.
- V.3 Gas handling system for the high purity He⁴ gas, used in the experiments in the He-II cell.
- V.4 Schematic of the electronics for measuring the characteristics of the superconductive tunnel junctions.
- V.5 Typical high-resolution trace of the second derivative (d^2v/dI^2) of the tunnel characteristic of an Al-Pb junction.



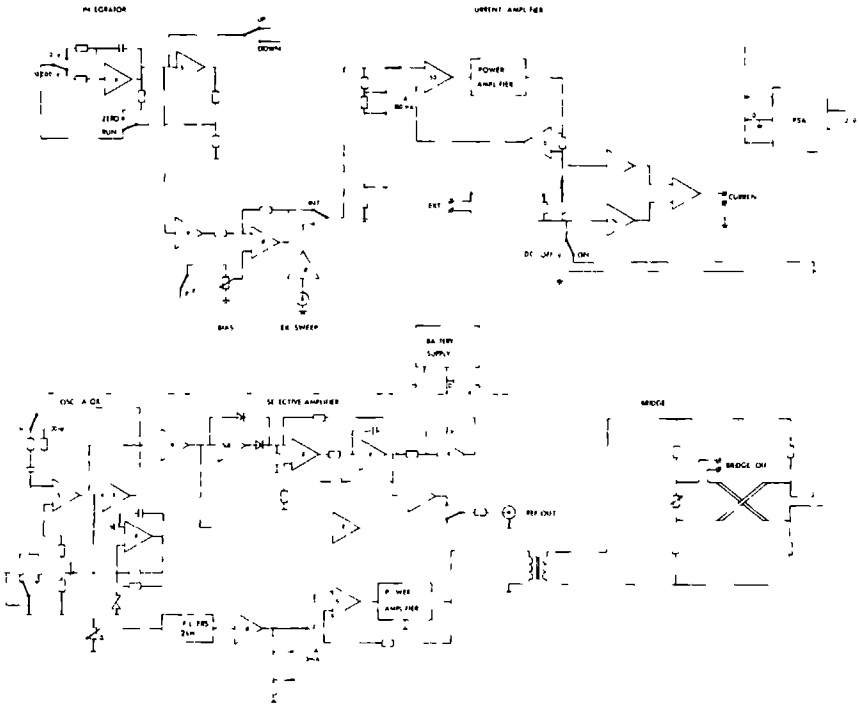
Calibration curve $R(T)$ of the Speer resistance thermometer used in the $\text{He}^3\text{-He}^4$ dilution refrigerator. Measuring power was less than 10^{-10} W. Nominal resistance at $T = 300$ K was 578Ω . For the calibration, the paramagnetic susceptibility of CMN was used, measured in a low-frequency AC susceptibility bridge. For details of the measuring circuit, see J.W.M. Bakker, Thesis, University of Nijmegen, 1973. The calibration of the thermometer was performed by H. van Kempen and H. Thuis.



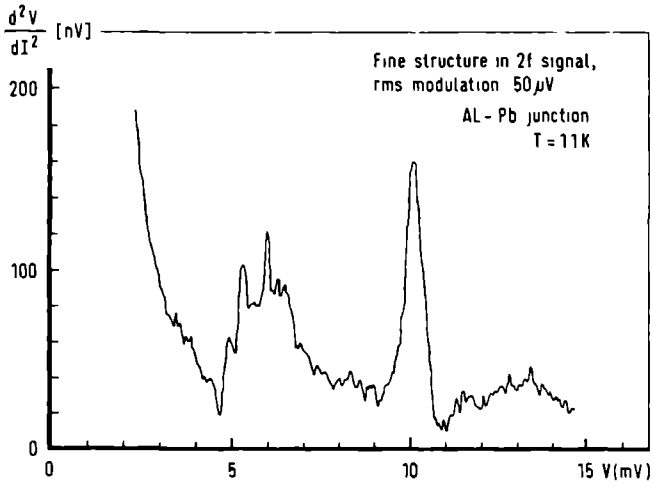
He³-He⁴ gas handling system of the dilution refrigerator.



Gas handling system for high-purity He^4 gas, used for the experiments with the He -II cell.



Schematic of the electronic apparatus, used for measuring the characteristics of the superconductive tunnel junctions. The main parts are the DC-current supply, the AC-current modulator and the resistive bridge circuit. For further details, see sec. III.2.1.



Typical high-resolution trace of the second derivative (d^2V/dI^2) of the tunnel characteristic of an Al-Pb junction. This curve was obtained with the tunnel electronics shown in V.4. (from: Th. Rasing, doktoraal-thesis, University of Nijmegen, 1976).

SUMMARY.

This thesis is concerned with experiments on the propagation of pulses of high-frequency phonons using evaporated thin metallic films as generators and detectors. The characteristics of these phonon transducers and the relevance of the investigated materials are reviewed briefly. The experimental techniques used for preparation and operation of the transducers, for detecting the pulse signals, and for attaining the required cryogenic conditions are discussed. Experimental results are given on phonon transmission in sapphire (Al_2O_3), using both broad-band (thermal) and narrow-band (monochromatic) phonon radiation. Transport of phonon pulses in superfluid Helium II with negligible thermal scattering is discussed. Also an experiment is described to study some properties of thin, superfluid Helium films, using fast evaporation of these films. In addition, we report on experiments of the transmission of phonon pulses through sapphire-liquid Helium interfaces at $T = 0.25$ K, under conditions of ballistic (interaction-free) energy transport in both materials forming the interface. These experiments provide a direct method to acquire information on the transfer of phonon energy from a solid into liquid Helium as function of: phonon polarisation (longitudinal or transverse), phonon frequency, and Helium pressure. Evidence is deduced for a down-conversion in energy of the phonons that have crossed the material interface.

Dit proefschrift behandelt experimenten betreffende het transport van korte pulsen van hoog-frekwente (100 - 500 GHz) acoustische energie (ultrageluid), fononen genaamd, waarbij gebruik gemaakt wordt van opgedampte dunne metallische films als zender en ontvanger. De eigenschappen van deze fononen-bronnen en het belang van de onderzochte materialen worden kort besproken in sec. II. Sec. III handelt over de experimentele technieken die gebruikt zijn voor de fabricage van deze dunne films, voor het detecteren van de puls-signalen en die voor het bereiken van de vereiste lage temperatuur.

De experimentele resultaten van het fononen-transport in saffier (Al_2O_3) worden gegeven in sec. IV.1, hierbij is gebruik gemaakt van acoustische straling met zowel een brede als een nauwe frekwentie-band. Het transport van fononen-pulsen in vloeibaar Helium-II, waarin verwaarloosbare verstoring optreedt als gevolg van de extreem lage temperatuur ($T = 0.1$ Kelvin) wordt behandeld in sec. IV.2. Eveneens wordt een experiment beschreven waarin enige eigenschappen van dunne superfluide helium films worden bepaald, door gebruik te maken van een snelle verdamping van deze films. In sec. IV.3 worden experimenten behandeld, die betrekking hebben op de transmissie van fononen-energie-pulsen door grensvlakken van een vaste stof (saffier) en vloeibaar Helium-II, op een temperatuur van $T = 0.25$ K, onder deze condities is er een storingsvrij transport van energie-pulsen binnenin beide materialen aan weerszijden van het grensvlak (ballistisch transport), zodat de effecten van de energie-transmissie in het grensvlak direct worden waargenomen. Deze overdracht wordt onderzocht voor verschillende polarisatie-richtingen van de acoustische energie en voor de afhankelijkheid van energie-dichtheid en hydrostatische druk in vloeibaar Helium.

CURRICULUM VITAE H.W.M. SALEMINK

- Geboren : 26 juli 1949 te Nijmegen
- 1961 - 1967 : Gymnasium B, Canisius College, Nijmegen
- 1967 : Begin studie Natuurkunde, K.U. Nijmegen
- sept. 1973 : Doctoraalexamen Experimentele Natuurkunde,
hoofdvak Vaste Stoffysica
- 1973 - 1979 : Promotie-onderzoek Experimentele Vaste Stoffysica,
afd. Experimentele Natuurkunde 4,
groepsleider: Prof.Dr. P. Wyder

STELLINGEN

1. De toepassing van ^{13}C kernspinresonantie via proton-ontkoppeling en magic angle spinning wordt bemoeilijkt om twee redenen: bij lage magneetvelden door de te geringe resolutie en bij hoge magneetvelden door het vereiste hoge toerental voor magic angle spinning.
V.I. Bartuska, G.E. Maciel, J. Schaefer en E.O. Stejskal, Fuel 56, 354 (1977).
2. De grote anomalieën in de specifieke weerstand boven de supergeleidende overgangstemperatuur van aluminium zijn geen intrinsieke eigenschappen van dit materiaal.
E. Zair, M. Sinviani, B. Levy en A.J. Greenfield, J. Physique (Paris) C6-496 (1978).
3. Akoustische paramagnetische resonantie (APR) aan gast-ionen in kristallen kan selectief zijn voor ionen in een vervormde potentiaal van een bepaalde symmetrie, de resultaten uit APR metingen kunnen daardoor afwijken van die, verkregen met andere methoden.
F.S. Ham, Phys. Rev. B 4, 3854 (1971), J.N. Lange, Phys. Rev. B 14, 4791 (1976).
4. De anisotropie van de lineaire magneto-weerstand in aluminium, gevonden door Kesternich, Uhlmeier en Schilling kan geheel verklaard worden uit de geometrie van de potentiaalkontakten.
W. Kesternich, H. Uhlmeier en W. Schilling, Phil. Mag. 31, 471 (1975).
5. Tengevolge van de onbekende achtergrondeffecten is het niet goed mogelijk om met een puntkontaktmethode de elektron-fonon wisselwerking te bepalen bij lage energien; het is mogelijk deze wisselwerking waar te nemen in een transversaal elektronfokusering-experiment.
I.K. Yanson, JLTP Letters 44, 148 (1976), V.S. Tsol, JETP Letters 19, 70 (1974).

6. Bij de interpretatie van absorptiemetingen van dunne metaalfilms in het verre infrarood moet men zich realiseren dat de veelgebruikte formule, zoals bijvoorbeeld gegeven door Tinkham, een veel beperkter geldigheidsgebied heeft dan meestal wordt aangenomen.
M. Tinkham, in: Optical Properties and Electronic Structure of Metals and Alloys (onder redactie van F. Abeles), North-Holland Publishing Company, Amsterdam (1966), p. 431.
7. De levensduren van aangeslagen toestanden in supergeleiders kunnen op direkte wijze gemeten worden met behulp van korte ver-infrarood stralings-pulsen.
8. De radiofrequentie storing, afkomstig van personenoproepinstallaties, maakt bepaalde experimenten welhaast onmogelijk; bij installatie van dergelijke apparatuur behoort tevens in adequate tegenmaatregelen voorzien te worden.
9. In de meeste gevallen is een kompas het best bruikbaar op geruime afstand van het anker.

Nijmegen, 14 juni 1979

H. Salemink.

